

Medizinische Fakultät der
Martin-Luther-Universität Halle-Wittenberg

**The influence of hyperoxia on intracellular reactive oxygen
species formation and antioxidant enzyme systems in
mouse lungs**

Dissertation
zum Erwerb des akademischen Grades
Doktor der Medizin (Dr. med.)

von Leonore Binder
geb. 06.08.1990 in Leipzig

Betreuerin: PD Dr. rer. nat. rer. medic. Babett Bartling
Gutachter*innen: PD Dr. rer. nat. rer. medic. Babett Bartling
PD Dr. rer. nat. Stefanie Endesfelder, Berlin
Prof. Dr. med. Jan-Henning Klusmann

01.12.2020
04.05.2021

Abstract

Preterm infants often require mechanical ventilation and supplemental oxygen administration due to lung immaturity. It is apparent that during induced hyperoxia an increased intracellular generation of reactive oxygen species (ROS) is caused in the exposed lung tissue. It is, however, still unclear which effect an external oxygen application has on the intrinsic formation of free ROS in lung tissue immediately after application or at a later time point. Therefore, my study aimed at the detection of free ROS formation and expression of selected antioxidant defence enzymes in lung tissue of mice treated with oxygen from birth.

Newborn C57Bl/6 mice were postnatally exposed to either moderate (50 % FiO₂) or severe (75 % FiO₂) hyperoxia in a self-constructed chamber for either short (\leq 120 min) or long (14 d) durations. Untreated mice were housed at physiologic oxygen conditions (20,9 % FiO₂). Assessment of free ROS (mainly \cdot O₂) formation via EPR technology or expression of important antioxidant enzymes (MnSOD, Cu/ZnSOD, catalase) via immunoblot technique was performed directly after treatment in newborn or infant (14 d) mice or when mice reached adulthood (60 d). In addition, selected general data of treated mice were recorded, including their physical activity in a running wheel.

The assessment of general data (body weight, lung-to-body weight ratio, lung weight wet-to-dry ratio, food and water consumption) and of running wheel activity did not show an adverse effect of the 14 d oxygen treatment on post-treatment development and health stage of mice. Comparative ROS analysis of cellular fractions isolated from lung tissue revealed that most free ROS formation occurs in the mitochondria-reduced cytoplasmic fraction. Moreover, total lung free ROS generation as well as the proportional cellular fractionated formation per lung tissue weight slightly changes with mouse age. Lungs of infant mice always showed less free ROS formation than lungs of newborn or young mice. Short-term treatment of newborn or infant mice with moderate or severe hyperoxia revealed a negative effect of oxygen on the internal free ROS formation earliest after 120 min of treatment. In addition, the lung cellular expression of antioxidant enzymes changes with mouse age. Catalase reached the maximum expression rate in murine lung tissue already at infant age, whereas MnSOD and Cu/ZnSOD are mainly expressed in young mice. Directly after the long-term treatment with oxygen for 14 d, the expression level of catalase was further increased in response to moderate hyperoxia, and of MnSOD in response to severe hyperoxia. These changes were not detectable in young mice 45 days after oxygen treatment. ROS analysis in total cell preparations of lung tissues showed only effects of moderate, but surprisingly not of severe hyperoxia on the internal free ROS formation. In detail, lungs of mice treated with moderate hyperoxia had lower intrinsic free ROS formation immediately after treatment, but higher free ROS formation at young age 45 days after treatment.

The intrinsic formation of free ROS and expression of antioxidant enzymes in mouse lung tissue is influenced by the postnatal development stage, as well as by a postnatal treatment with oxygen depending on the extent of hyperoxia. However, the levels of antioxidant enzymes and free ROS formation do not correlate, which again suggests the influence of multiple factors on the internal formation of ROS in the postnatal lung.

Referat

Aufgrund pulmonaler Unreife benötigen Frühgeborene häufig eine apparative Beatmung, sowie zusätzliche Sauerstoffgaben. Es ist bekannt, dass die dadurch induzierte Hyperoxie eine gleichzeitige erhöhte intrazelluläre Bildung von reaktiven Sauerstoffspezies (ROS) bedingt. Allerdings ist noch unklar, welchen Effekt die externe Sauerstoffgabe direkt nach der Behandlung oder zu einem späteren Zeitpunkt auf die intrinsische Produktion von freien ROS in Lungengewebe hat. Daher untersucht meine Studie die Bildung freier ROS und die Expression ausgewählter antioxidativer Abwehrenzyme im Lungengewebe von Mäusen, welche postnatal mit Sauerstoff behandelt wurden.

Neugeborene C57/Bl6 Mäuse wurden postnatal in einer selbstkonstruierten Kammer entweder moderater (50 % FiO₂) oder schwerer (75 % FiO₂) Hyperoxie über kurze (<120 min) oder lange (14 d) Dauer ausgesetzt. Unbehandelte Mäuse wurden unter physiologischen Sauerstoffbedingungen (20,9 % FiO₂) aufgezogen. Die Untersuchung freier ROS-Bildung (hier hauptsächlich 'O₂') mittels ESR-Methode, bzw. der Expression von wichtigen antioxidativen Enzymen (MnSOD, Cu/ZnSOD, Katalase) mittels Immunblot-Methode bei neugeborenen oder kindlichen (14 d) Mäusen erfolgte direkt nach Behandlung, oder sobald diese das Erwachsenenalter erreichten (60 d). Zusätzlich wurden ausgewählte allgemeine Daten der behandelten Mäuse erhoben, welche deren physische Aktivität im Laufrad einschlossen.

Die Untersuchung der allgemeinen Daten (Körpergewicht, Verhältnis Lungen-zu-Körpergewicht, Verhältnis Lungengewicht feucht-zu-trocken, Futter- und Wasserverbrauch) und der Laufradaktivität zeigten keinen negativen Effekt der 14-tägigen Sauerstoffbehandlung auf die postinterventionelle Entwicklung und den Gesundheitszustand der Mäuse. Vergleichende ROS-Analysen der Zellfraktionen, welche aus dem Lungengewebe isoliert wurden, zeigten, dass die meiste freie ROS-Bildung im Mitochondrien-reduzierten Zellplasma erfolgt. Darüber hinaus ändert sich mit dem Alter der Tiere sowohl die Gesamt ROS-Produktion, als auch diese in den einzelnen Zellfraktionen. Die Lungen von infanten Mäusen zeigten stets weniger ROS-Produktion als die Lungen von jungen oder adulten Tieren. Die Kurzzeitbehandlung von neugeborenen oder infanten Mäusen mit moderater oder schwerer Hyperoxie zeigte einen negativen Effekt des Sauerstoffs auf die intrinsische Bildung von freien ROS frühestens nach 120 Minuten Behandlung. Außerdem ändert sich die pulmonale zelluläre Expression von antioxidativen Enzymen mit zunehmendem Alter der Mäuse. Katalase erreichte die maximale Expressionsrate in murinem Lungengewebe bereits im Kindesalter, wohingegen MnSOD und Cu/ZnSOD hauptsächlich in jungen Mäusen exprimiert werden. Direkt nach der Langzeitbehandlung mit Sauerstoff über 14 Tage wurde das Expressionslevel von Katalase in Reaktion auf moderate, und das von MnSOD in Reaktion auf schwere Hyperoxie weiter gesteigert. Diese Veränderungen waren in jungen Mäusen 45 Tage nach Sauerstoffgabe nicht mehr nachweisbar. Die ROS-Analysen von Gesamtzelllysaten der Lungengewebe zeigten nur eine Wirkung von moderater, aber überraschenderweise nicht von schwerer Hyperoxie auf die intrinsische Produktion von freien ROS. Genauer gesagt zeigten die Lungen von Mäusen, welche mit moderater Hyperoxie behandelt wurden, eine geringere intrinsische ROS-Produktion direkt nach der Behandlung, aber im jungen Erwachsenenalter, 45 Tage nach Behandlung, eine höhere ROS-Produktion.

Die intrinsische Bildung von freien ROS, sowie die Expression von antioxidativen Enzymen in Mauslungen wird sowohl vom postnatalen Entwicklungsstand, als auch von vorhergegangener Sauerstoffbehandlung beeinflusst, dies ist abhängig vom Ausmaß der Sauerstoffbehandlung. Allerdings korrelieren die Level der antioxidativen Enzyme und die Produktion von freien ROS nicht direkt, was wiederum den Einfluss von multiplen Faktoren auf die intrinsische ROS-Produktion in der postnatalen Lunge vermuten lässt.

Contents

Figures.....	III
Tables.....	IV
Abbreviations.....	V
1. Introduction.....	1
1.1 Premature birth and lung development.....	1
1.1.1 Lung development in humans.....	1
1.1.2 Situation in preterm infants.....	3
1.1.3 Animal models for lung development.....	4
1.2 Importance of oxygen.....	4
1.2.1 Biochemical background.....	4
1.2.2 Clinical use.....	5
1.2.3 Adverse effects of oxygen.....	5
1.3 Coherence of lung altering and physical activity.....	6
1.4 Reactive oxygen species (ROS) and antioxidant systems.....	7
1.4.1 Sources of ROS and their intracellular role.....	7
1.4.2 Pathological effects of ROS.....	8
1.4.3 Antioxidant systems	8
1.4.4 Measurement methods for ROS.....	10
2. Aim of work	12
3. Material and Methods.....	13
3.1 Biological methods.....	13
3.1.1 Laboratory mice and experimental set-up.....	13
3.1.2 Oxygen treatment.....	14
3.1.3 Recording of voluntary physical activity.....	15
3.1.4 Monitoring of nutrition.....	16
3.1.5 Dissection and sample preservation.....	16
3.2 Biochemical methods.....	18

3.2.1 Sample preparation	18
3.2.2 Electron paramagnetic resonance (EPR) spectroscopy.....	20
3.2.3 Protein quantification.....	21
3.2.4 SDS polyacrylamide gel electrophoresis (SDS-PAGE) and immunoblot de- tection.....	21
3.3 Statistics.....	23
4. Results.....	24
4.1 General data of mouse groups.....	24
4.1.1 Effect of hyperoxia on running wheel activity and nutrition.....	26
4.2 Results of biochemical analyses.....	28
4.2.1 Influence of age and hyperoxia on cellular protein levels.....	28
4.2.2 Characterisation of fractionation of cellular compartments.....	29
4.2.3 Effect of short-term oxygen treatment.....	33
4.2.4 Effect of age and long-term oxygen treatment on free ROS formation.....	35
4.2.5 Effect of age and long-term oxygen treatment on antioxidant systems.....	36
5. Discussion.....	38
5.1 Influence of hyperoxia on free ROS formation and anti- oxidant enzymes.....	38
5.2 Influence of hyperoxia on voluntary physical activity.....	40
5.3 Technical aspects of murine hyperoxia trials.....	41
5.4 Conclusion and outlook.....	42
6. Summary.....	43
7. Literature.....	44
8. Theses.....	50
Erklärungen.....	VII
Danksagung.....	VIII

Figures

Figure 1: Schematic presentation of the human and murine lung development	2
Figure 2: EPR signal determination.....	11
Figure 3: Study set-up for hyperoxia trial.....	14
Figure 4: Self-constructed oxygen treatment unit and wheel running station.....	15
Figure 5: Sample preparation of mouse lung lobes.....	18
Figure 6: Protein sample preparation in cellular fractions for free ROS analysis (a).....	20
Figure 7: Mean running distance, mean running velocity and average number of breaks per day	28
Figure 8: Cellular protein content per lung wet tissue weight.....	29
Figure 9: Qualitative protein analysis of cellular fractions	30
Figure 10: Absolute protein content of cellular fractions isolated from mouse lung tissue depending on age.....	31
Figure 11: Free ROS formation in cellular fractions per protein or lung wet tissue in untreated infants (study group B).....	32
Figure 12: Free ROS formation in cellular fractions per different age groups.....	33
Figure 13: Free ROS formation in mt-enriched organelle fraction and mt-reduced cytoplasm after short-term mH ventilation in newborn and infant mice per untreated newborn (study group A).....	34
Figure 14: Free ROS formation in mt-enriched organelle fraction and mt-reduced cytoplasm after short-term mH and sH ventilation in newborn mice per untreated newborn (study group A).....	34
Figure 15: Free ROS formation in mouse lung tissue depending on age and long-term oxygen treatment.....	35
Figure 16: Protein expression of selected antioxidant defence enzymes dependent on age and long-term oxygen treatment of mice for CuZnSOD, MnSOD and catalase.....	37

Tables

Table 1: Measuring methods for cellular free ROS formation.....	10
Table 2: Study group A: general data of newborn and infant mice treated with short-term hyperoxia (10 - 120 min).....	24
Table 3: Study group B: General data of infant mice treated with long-term hyperoxia	25
Table 4: Study group C: General data of young mice treated with long-term hyperoxia and subsequent normoxia	25
Table 5: Study group D: General data of young mice provided with running wheels for 30 days.....	26
Table 6: Nutritional and running wheel parameters of young mice provided with running wheels for 30 days (study group D).....	26

Abbreviations

$\cdot\text{CP}$	3-carboxy-proxyl radical
$\cdot\text{O}_2^-$	superoxide radical
AB	amidoblack
ANOVA	One Way Analysis Of Variance test
APS	ammonium peroxydisulfate
ATP	adenosine triphosphate
AUC	area under curve
BAL(F)	bronchoalveolar lavage (fluid)
BCA	bicinchoninic acid
BSA	bovine serum albumine
CP-H	1-hydroxy-3-carboxy-pyrrolidine
CuZnSOD	copper zinc superoxide dismutase
d	day
DFO	deferoxamine mesylate
DTT	dithiothreitol
EGTA	ethylene glycol-bis(2-aminoethylether)- <i>N,N,N',N'</i> -tetraacetic acid
EPR	electron paramagnetic resonance
Fe^{3+}	iron(III)
FiO_2	fraction of inspired oxygen
free ROS	relative ROS molecules after scavenging and elimination
GAPDH	glyceraldehyde 3-phosphate dehydrogenase
h	hour(s)
H_2O bidest	double-distilled water
H_2O_2	hydrogen peroxide
HCl	hydrochloric acid
HEPES	2-[4-(2-hydroxyethyl)piperazin-1-yl]ethanesulfonic acid
HRP	horseradish peroxidase

KCl	potassium chloride
mH	moderate hyperoxia treatment group
min	minute(s)
MnSOD	manganese superoxide dismutase
mt	mitochondria
N	normoxia treatment group
Na ₂ -EDTA	di-sodium ethylenediaminetetraacetate
NaCl	sodium chloride
p	probability value
PBS	phosphate buffered saline
PBS-T	PBS solution with 0.1 % Tween
PEX	peroxisomal membrane protein
ROS	reactive oxygen species
SaO ₂	capillary oxygen saturation
SD	standard deviation
SDS	sodium dodecyl sulfate
SDS-PAGE	sodium dodecyl sulfate polyacrylamide gel electrophoresis
SE	standard error
sH	severe hyperoxia treatment group
SI	signal intensity
TEMED	<i>N,N,N',N'</i> -Tetramethylethane-1,2-diamine
Tris	2-Amino-2-(hydroxymethyl)propane-1,3-diol
V	volt
w	week(s)

1. Introduction

1.1 Premature birth and lung development

1.1.1 Lung development in humans

Adequate capabilities for gas exchange and blood oxygenation determine life in aerobic surroundings. The steady development and growth of the complex human lung structure begins during the early embryonic period and continues into childhood [1]. Four characteristic periods can be determined over the course of the human pregnancy, with some overlap at the beginning and end of each period (Figure 1 *above*). The embryonic period lasts from conception until week 6 of gestation. Lung organogenesis starts as a ventral bud of the oesophagus and subsequently, lobar and segmental portions of the airway tree are preformed. In the pseudoglandular period (6 - 16 weeks), the creation of conducting airways starts, reaching the level of the acinus. Also, the completion of the basic vascular development is reached. In the following canalicular period (16 - 24 weeks), the early development of pulmonary parenchyma takes place with the differentiation of alveolar type (AT) I and II cells and the multiplication of vascular capillaries. Together with flattening of the alveolar epithelial cells, this allows the formation of a thin blood-air-barrier. Around the 26th week of gestation, the first localised secretion of surfactant begins. The surfactant system is one of the last endogenous systems to develop before birth, it normally matures between 29 and 32 weeks of gestation. It plays a pivotal role in lung functionality by reducing the surface tension in the alveolar air-liquid-interface and hereby later preventing ventilated alveoli from collapsing. Only during the saccular period (24 weeks until term at around 40 weeks), starting from the 32nd week, the actual formation of first alveoli initiates the distribution of functional respiratory tissue. The expansion and growth of blood vessels, as well as a natural increase in fetal concentrations of cortisol are characteristic for this period.

After these developmental sections, which were generally agreed on by the International Congress of Anatomists meeting in Leningrad in 1970, a fifth, mostly postnatal period affiliates [1]. This so-called alveolar period is expected to last from around 36 weeks of gestation (the first manifestation of true respiratory alveoli) up to around 2 years of age. Until then, the complex alveolarisation of lung parenchyma is almost completed concerning size of respiratory surface, number of alveoli, vascular and microvascular structure and overall relative size of structures. However, a study using modern helium mag-

netic resonance could show that lung volume and alveolar size continue to increase in a population of children and adolescents of 7 to 21 years of age [2]. This indicates that research on human lung development still is not yet fully clarified today. Murine lung development differs from that of humans concerning duration and stage of development at birth (Figure 1 *below*).

By the time of birth and disconnection from the umbilical cord, fetal respiratory gas exchange can no longer be performed by the placenta, therefore lungs have to take over. Depending on fetal age and lung developmental status at birth, more or less severe respiratory impairment is imminent in preterm delivery.

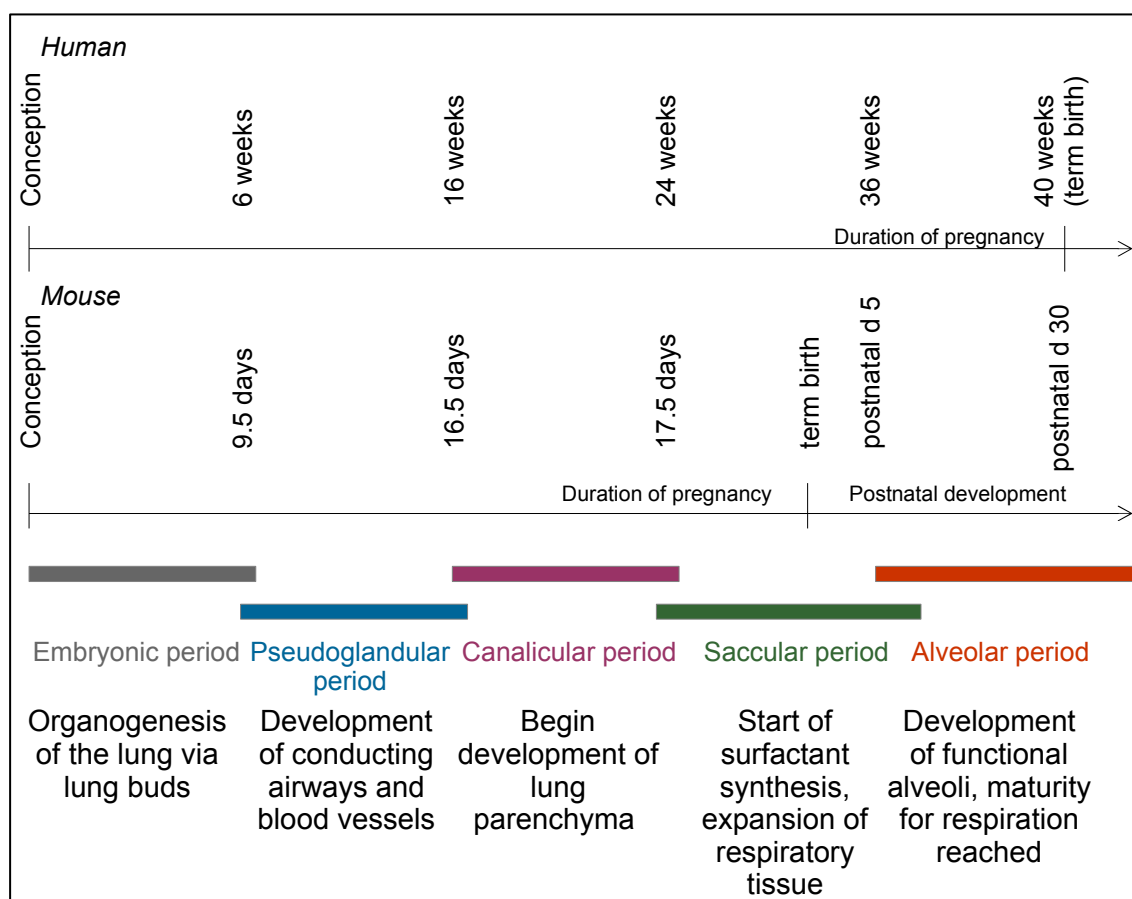


Figure 1: Schematic presentation of the human and murine lung development

The average pregnancy lasts for 37–42 weeks in humans and 19–21 days in mice from conception until term birth. Lung development is categorised in five overlapping time periods, starting from conception and completed during adolescence. As opposed to humans, murine offspring is already born during the saccular period of lung development.

Modified after Smith et al. [1] and Chao et al. [3].

1.1.2 Situation in preterm infants

Premature birth interrupts the normal lung development [1]. Affected neonates have underdeveloped lungs and very often require assistance to maintain adequate respiration. In humans, prematurity is defined as birth before 37 weeks of gestation or at a birth weight of under 2500 g. It can be subdivided into extremely preterm (22 - 27 weeks of gestation), very preterm (28 - 31 weeks) and moderately preterm (32 - 36 weeks). When born between 24 to 32 weeks of gestation, the infant's lung is in the saccular period of development. That implies, at this time point, the division of the primitive alveolar sacs into mature alveoli has not yet begun and the proliferation of the capillary network is still incomplete. Immature surfactant and cortisol systems add to the risk for emergence of respiratory distress [4].

Preterm births accounted for 11.1 % of live births worldwide and 8.6 % in developed countries in 2010 and global numbers have inclined by 14.7 % since 1990 [5]. Effective actions have been taken in terms of improvement of perinatal care in recent years [6 – 8], which noticeably decreased morbidity and mortality of infants born prematurely. Nevertheless, 40 % of all neonatal deaths in Europe are constituted by babies born extremely preterm (before 28 weeks of gestation or under 1000 g birth weight) [9]. Only about 1 to 1.5 % of all live births are defined as very preterm, but these infants still account for one third to half of all neonatal deaths [9].

Significant increase in live birth rates of extremely preterm infants can be observed in recent decades for some countries [6], whereas the European Perinatal Health Report (EPHR) 2010 showed a trend towards stagnation of increasing numbers within Europe between 2004 and 2010 (for review [10]). Extremely preterm infants are increasingly delivered at high-level hospitals or transferred in utero in case of imminent birth, and treated with evidence-based therapy [6]. The centralised treatment of preterm neonates in highly specialised neonatal care centres improved survival rates, but also increased the number of patients with potential long-term impairment that may require further health services and social assistance [6]. Further research on long-term consequences of extremely preterm birth as well as precautionary and predictive measures is needed.

The smallest and most preterm infants are still at high risk of death [9] or the development of chronic diseases associated with respiratory impairment, such as asthma, bronchopulmonary dysplasia or COPD later in life (for review [11]). Chances of survival increase with higher gestational age and administration of surfactant [6]. Strategies that accelerate lung development and assist in providing adequate gas exchange are quite advanced and updated constantly. They include the antenatal administration of corticosteroids to the mother, the intra-bronchial application of surfactant postpartum, as

well as the introduction of gentler ventilation techniques and reduction of administered oxygen concentrations [12, 13].

1.1.3 Animal models for lung development

Studies concerning human lung development and the effects of hyperoxia are necessary, but tissue sample collection is difficult and restricted due to ethical reasons. Therefore, numerous studies have been carried out in different animal models: lambs [14], baboons [15], pigs [16] and rabbits [17], but models in rats and mice remain the most common. Rodents proved to be particularly suitable for studies on preterm birth, because their offspring are physiologically born during the sacular period of lung development [3, 18] (see Figure 1 *below*). Newborn mice start their alveolar development around postnatal day 4 and eventually complete the sacular period by day 14 [19]. In that way, a 'premature birth' according to human standards coincides with the murine model and postnatal oxygen treatment is administered during the vulnerable phase of development. Also, their reproduction cycle is comparably short, which is supportive for laboratory trials.

1.2 Importance of oxygen

'Good and evil we know in the field of this world grow up together almost inseparably.' *Paradise Lost* (John Milton; 1608–1674)

1.2.1 Biochemical background

Atmospheric oxygen is essential for multicellular eukaryotic life forms, as the aerobic metabolism is the most effective energy source currently known. It is executed mainly in the mitochondria through oxidative phosphorylation, where nutritional components like glucose, fatty acids or amino acids get combusted into bioavailable energy reservoirs, such as adenosine triphosphate (ATP). The energy balance of oxidative phosphorylation is generally more efficient than under anaerobic circumstances.

Mammals have developed effective mechanisms to compensate for the physiological intrauterine hypoxia during fetal development. Increased oxygen affinity of the fetal haemoglobin combined with significantly higher cardiac output ensure adequate tissue oxygenation [8]. Additionally, placental oxygen levels vary between the different stages of pregnancy to coordinate growth and preparation for extrauterine life [20].

1.2.2 Clinical use

Concentrated gaseous oxygen has become one of the most frequently administered pharmaceutical treatments in emergency and respiratory care for critically ill patients. Due to inefficient gas exchange in preterm neonates with underdeveloped alveolar systems, the external application of additional oxygen together with high pressure mechanical ventilation became a convenient, effective and widely used therapeutic option. It plays a pivotal role in the improvement of survival and morbidity rates in these patients in danger of developing a severe respiratory distress syndrome. Treatment regimes for premature infants have greatly improved in recent years concerning mechanical ventilation techniques and applied oxygen concentrations to reduce the resulting structural damage to lung tissue. With improving monitoring techniques, the focus increasingly lies on target capillary O_2 saturation (SaO_2) and titrated adjustment of the fraction of inspired oxygen (FiO_2), rather than previously used fixed FiO_2 schemes (for review [7, 8, 21]).

Despite its generally known potential for damage, oxygen remains one of the standard drugs in many diseases affecting alveolar gas exchange. Even after successful resuscitation, 36 % of infants born at a gestational age of ≤ 25 weeks were discharged from the hospital on home oxygen therapy for a median length of 2.5 months, with longest durations lasting into adolescence [7].

1.2.3 Adverse effects of oxygen

Although it is such a commonly administered medication and simply essential for aerobic life, oxygen will cause tissue damage when administered above a certain dosage, which is mainly mediated through the formation of reactive oxygen species (for review [22, 23]). The external application of oxygen, and thereby triggering of tissue hyperoxia, can cause oxidative stress in newborns [16, 24], but corresponding mechanisms are not yet fully understood. Oxidative stress is defined as the 'imbalance between oxidants and antioxidants in favour of the oxidants', potentially leading to molecular damage [25]. Surprisingly, the lethality of superphysiologic oxygen administration ($> 95\%$ FiO_2) was found to be higher in adult animals than in newborns of many species such as rabbits, rats and mice [26–28]. This was suggested to be caused by inadequate cellular antioxidant enzyme induction after infancy [27, 29].

Premature infants with impaired respiratory function upon birth very often require assisting mechanical ventilation with elevated FiO_2 levels for adequate gas exchange, often as high as 80 % FiO_2 over longer periods of time (for review [7, 21]). This thera-

peutic regimen is known to have a severe impact on the extrauterine alveolar and vascular lung development. Structural changes in lung morphology are traced back to exaggerated neonatal O₂ treatment in animal models [18, 30]. Clinical observations in human infants are difficult due to multifactorial influences, but a hyperoxia-induced impairment of lung development is generally assumed (for review [22]). High levels of administered oxygen gas were shown to increase indirect markers of oxidative stress in blood samples of premature infants [24].

1.3 Coherence of lung altering and physical activity

Research on the relation between structural lung injuries associated with prematurity and voluntary physical activity later in life is limited and conclusions differ widely. Some clinical studies did not find any evidence for the connection between neonatal severe respiratory distress, followed by structural lung changes and the later physical performance in children at school age [31]. Others found clear exercise limitations in survivors of bronchopulmonary dysplasia, a condition concerning structural lung changes following prolonged mechanical ventilation and oxygen supplementation [32]. Their probands reported reduced exercise participation and experienced mild exercise-induced bronchospasm with accompanying hypoxemia, which they found to be due to impaired gas exchange and subsequent reduction in SaO₂ during exercise. In 2008, Smith et al. examined former preterm infants with and without developed bronchopulmonary dysplasia for their exercise capacity at school-age. They found mild small-airway obstruction, gas trapping, and a disproportionately impaired exercise capacity compared to the degree of airflow limitation [33]. On the other hand, a retrospective study found children, who previously were very low birth weight preterm infants, to be slightly more physically active on voluntary basis than children in a control group [34].

Regarding animal studies, only one paper analysed the effect of hyperoxia-induced lung injury onto the exercise capacity of rodents. In their study rat pups were treated with 95 % FiO₂ over 14 days and their run distance assessed via forced treadmill running [35]. Experimental assessment of solely voluntary physical activity after postnatally administered isolated hyperoxia treatment is missing at the time of my research. However, some studies looked at the influence of physical exercise onto prevention, progression and recovery from previous lung injuries in animal models. One experiment suggested that physical exercise may, at least partially, prevent the oxidative damage caused by experimentally induced lung injury in rats [36]. Another study found that regularly performed moderate (forced) exercise increased the tissue antioxidant defence in rat tissues [37].

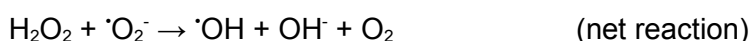
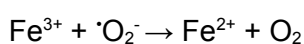
1.4 Reactive oxygen species (ROS) and antioxidant systems

1.4.1 Sources of ROS and their intracellular role

Hier Text eingeben

Reactive oxygen species (ROS) define a variety of highly active molecules that contain oxygen and are generated as by-products of normal aerobic cellular metabolism. They exist ubiquitously in eukaryotic cells and biologic systems and, depending on the species and cellular environment, have a lifetime of nanoseconds to seconds [38]. The initial step in ROS formation is the generation of the superoxide anion radical ($\cdot\text{O}_2^-$) by single electron transfer onto molecular oxygen (O_2), for example from the mitochondrial electron transfer chain. The enzymatic dismutation of $\cdot\text{O}_2^-$ produces hydrogen peroxide (H_2O_2), a stable non-radical molecule able to cross cell membranes, which can be reduced enzymatically to water and O_2 . In the presence of iron, non-disposed coexisting H_2O_2 and $\cdot\text{O}_2^-$ molecules interact to generate hydroxyl radicals ($\cdot\text{OH}$) in the Haber-Weiss reaction [39] (see below). This is one of the most aggressive and destructive radicals formed and thought to be responsible for oxidative cellular damage [40].

Haber-Weiss reaction:



Mitochondria - precisely the respiratory chain - are thought to be the main supplier of ROS within somatic cells through constant electron leakage [41]. But also the reactions of xanthine oxidase, NADPH oxidase, cyclooxygenases, lipoxygenases, monoamine oxidase and cytochrome P450 complex are known to be (extramitochondrial) sources of $\cdot\text{O}_2^-$ and H_2O_2 (for review [42, 43]).

Peroxynitrite (ONOO^-), which is formed by combination of nitric oxide (NO^\cdot) with free oxygen radicals, adds to the cellular radical species as reactive nitrogen species (RNS). ROS are furthermore capable of rapidly inactivating NO^\cdot , which itself regulates numerous cellular or tissue reactions [14].

Although ROS regularly damage intra- and extracellular molecules in adverse effects or during apoptotic mechanisms, they usually serve a physiological role in eukaryotic organisms. ROS have an important impact as ubiquitous and powerful second messen-

gers, their signalling targets and mediated reactions are various and by far not yet fully understood [38]. There is growing evidence that ROS regulate signal transduction pathways which control gene expression and posttranslational protein changes, and are involved in immunity, cell function, growth, differentiation, ageing and apoptosis [13, 42, 44].

1.4.2 Pathological effects of ROS

It is generally assumed that treatment with elevated oxygen levels (F_{iO_2}) in respiratory air is increasing oxidative stress in multiple organ systems, especially the lung [12, 16, 24]. This is mainly due to the formation of reactive molecules in connection with aerobic cellular metabolism. Molecular oxygen is a willing and ubiquitously available acceptor of free electrons generated in several cellular processes. Excessive ROS production or insufficient endogenous antioxidant capacity result in oxidative stress, which is connected to a wide variety of pathologies (see [38]). A predominance of oxidants in biological systems causes direct or indirect damage to molecules, such as lipids, proteins and DNA, which can lead to cell injury or altered cell proliferation [45]. Also, ROS are linked to the release of proinflammatory mediators and hence the promotion of inflammation, which results in secondary tissue damage [46].

Nevertheless, too little ROS production or predominant antioxidant activity, a state called 'reductive stress', has also been linked to certain pathologies caused by protein aggregations (for review [47]). So in order to enable healthy multicellular life in aerobic conditions, the maintenance of an oxidant-antioxidant balance is indeed crucial.

1.4.3 Antioxidant systems

Tissue hyperoxia is enhancing the intracellular formation of superoxide molecules and subsequent production of further ROS. If the disposal is not sufficient, emerging hydroxyl radicals will cause molecular damage.

Control and elimination of excess intracellular ROS are performed by complex enzymatic and non-enzymatic antioxidant systems that contribute to the maintenance of the redox equilibrium. Superoxide dismutases account for the primary antioxidant enzyme system by catalysing the instant dismutation of $\cdot O_2^-$ into H_2O_2 and O_2 and hereby preventing the coexistence of both molecules. They were first described by McCord and Fridovich in 1969 [48]. Three types of SODs with different localisations are known:

- Copper zinc SOD (CuZnSOD, SOD1), located in the cytoplasm
- manganese SOD (MnSOD, SOD2) located in the mitochondrial matrix
- extracellular SOD (EC-SOD, SOD3), located extracellularly, but also known to be primarily cytoplasmic in newborns [49]

Further antioxidant enzymes then catalyse the subsequent degradation of hydrogen peroxide (H_2O_2) into H_2O in a second step of ROS defence, in order to avoid toxic accumulation. These include the families of peroxiredoxins, thioredoxins and glutathione peroxidases, as well as catalase [13, 50], for review [51]. Catalase is the main enzyme for reduction of H_2O_2 in eukaryotic cells and is found in the peroxisomal matrix. Glutathione peroxidases (GPX) use the reduced form of glutathione (GSH) to eliminate H_2O_2 by producing oxidised glutathione disulfide (GSSG) in the cytoplasm, which is then reduced again by glutathione reductase. The activity of enzymatic antioxidants is complemented by non-enzymatic antioxidants such as vitamins, polyphenols, glutathione and coenzyme Q10 [50]. The amount of detectable oxygen radicals is dependent on protein-related ROS formation and scavenging within the cellular compartments.

It is assumed that in preterm infants the antioxidant defence is less developed compared to term babies and therefore unable to react with the adequate increase in synthesis of antioxidants as a response towards hyperoxia or other oxidant challenges (for review [52]). It could have been shown that the antioxidant enzyme defence activity of the neonate (catalase, GPX and CuZnSOD) was significantly higher in full term neonatal umbilical cord blood compared to preterm newborn humans [53]. Also, catalase and SOD activity was found to increase throughout progressing pregnancy in homogenates of placentae and fetal liver [54]. Although valuable compensatory mechanisms for the relatively hypoxic intrauterine conditions were detected [8] (see chapter 1.2), preterms are thought to be protected less effectively against the oxidative damage of relative or absolute hyperoxic postnatal surroundings.

Numerous research can be found on fetal antioxidant enzyme development, but less data exists regarding the postnatal maturation of antioxidant systems and adaptation to external hyperoxia. It could be shown previously that cellular GPX and MnSOD expression in mouse lungs were higher at 21 and 56 days postnatally compared to date of birth, but CuZnSOD expression increased only 56 days after birth [28, 29].

1.4.4 Measurement methods for ROS

The measurable cellular ROS production results from the absolute formation of ROS molecules minus immediate scavenging and elimination and will below be termed as free ROS formation.

Several measuring methods have been proposed for the detection of free ROS formation (Table 1). Indirect methods assess the footprints of oxidative stress, which are more or less stable end products of interactions between ROS and nucleic acids or lipids. They include the detection of products from lipid peroxidation (thiobarbituric acid method or malonyl dialdehyde in blood), oxidative carboxylation (OxyBlot™ Kit) heme-oxygenase-1 mRNA, immunohistochemical staining for nitrotyrosine [12] and desoxyribose degradation products [55]. Also, high-performance liquid chromatography and mass spectrometry can be used to detect advanced oxidative protein products or isoprostanes as markers of oxidative stress [24]. Most of the footprint methods require time-consuming in vitro sample preparation, some are not specific or do not form stable analysis products.

A few methods have been developed to detect and quantify the production of ROS in intact cells or even living animals. This would enable the detection of direct external influences on ROS formation, such as through hyperoxia. These include small-molecule fluorescent ROS probes and protein-based fluorescent indicators, for example dihydroethidium which is selective for $\cdot\text{O}_2^-$ [56]. However, most of them still show disadvantages concerning for example selectivity, reversibility and compartment-targeting properties [38]. Several advanced methods for the direct measurement of radical formation in situ use spin traps, e.g. 5,5-dimethylpyrroline-1-oxide (DMPO) [57], alpha-phenyl N-tert-butyl nitron (POBN) [58] or 1-hydroxy-3-carboxy-pyrrolidine (CP-H) [59, 60].

Table 1: Measuring methods for cellular free ROS formation

Methods	Sample	Advantages	Disadvantages
indirect	in situ	<ul style="list-style-type: none"> reliable oxygenation footprint assessment 	<ul style="list-style-type: none"> unspecific to ROS molecules time-consuming
direct	in vivo	<ul style="list-style-type: none"> real-time ROS measurements direct effect of external stimulation or inhibition detectable 	<ul style="list-style-type: none"> partly unspecific to ROS molecules unreliable reversibility
	in situ	<ul style="list-style-type: none"> mostly specific to ROS molecules 	<ul style="list-style-type: none"> no direct assessment of external influences due to sample preparation

Intracellular processes of adaptation to hyperoxic conditions and the associated effect of hyperoxia onto the endogenous production of ROS are still unknown. Therefore, I measured the formation of free ROS in lung tissue via electron paramagnetic resonance (EPR) method. CP-H (1-hydroxy-3-carboxy-pyrrolidine) has been proved to be an adequate spin trap marker for intracellular free ROS formation [59, 60]. Its oxidation to \cdot CP mainly by electron donation from \cdot O₂⁻ [59], but also by \cdot OH [60] - delivered from the Fenton reaction - can be easily monitored by EPR spectroscopy (see Figure 2). Therefore, the spectrometer device applies an external magnetic field and subsequently measures the microwave absorption levels of the probe. These result from the permanent magnetic moment inherent to organic radicals such as \cdot OH and are directly dependent on the concentration of the contained oxidant [60].

Persistent storage on ice during the sample preparation process, as well as time synchronisation of measurements are crucial for comparable results to minimize early intracellular ROS formation. Over time of analysis, periodic readings are performed and the signal amplitudes noted. Preliminary studies showed that the signal intensity of free ROS formation in defrosting tissue homogenates gradually increases over time. A period of constant linear gain was determined for approximately one hour of intermittent readings. The final values for free ROS signalling resulted from this time-dependent linear gain in the paramagnetic amplitude of EPR signal. EPR signal is synonymous to the microwave absorption levels of \cdot CP over time. It gives an objective about the intracellular redox balance of the respective tissue sample as the detection of free ROS molecules is proportional to the absolute formation less the cellular antioxidant capacity. This linear gain required a normalisation to a stable cellular parameter in direct correlation to generation and scavenging of free ROS for which total protein content appeared optimal (see chapter 4.2.2.).

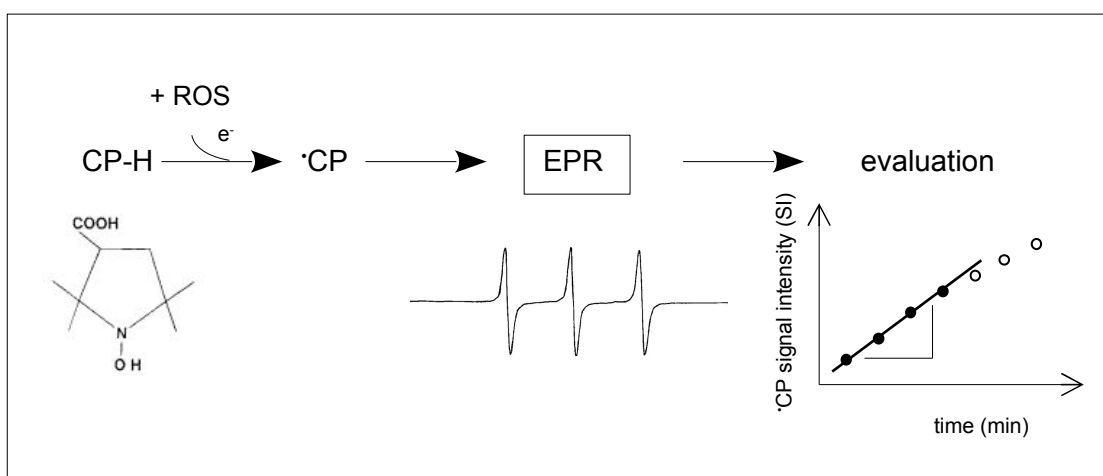


Figure 2: EPR signal determination

The spin trap CP-H accepts a single electron from a reactive oxygen species and hereby transforms into a radical. In the EPR spectrometer, the specific microwave absorption amplitudes are detected and mean values applied in a graph. The signal intensity of intracellular free ROS formation increases over time and shows a linear gain within a defined time period.

2. Aim of work

Detection of the absolute formation rate of intracellular free ROS in tissue cells is difficult due to their constant immediate elimination through scavenging processes and antioxidant enzyme activity. It is known that under induced hyperoxia increasing amounts of free ROS are apparent in tissues, but it is not yet clear, how the cell's internal production rate is affected by this treatment. Since oxygen is a frequently used element of therapy in preterm newborns, my study aimed at the analysis of free ROS formation as well as the expression of essential antioxidant enzymes in lung tissue immediately after oxygen treatment and also at a later time point by use of an established neonatal mouse model.

3. Material and Methods

3.1 Biological methods

All procedures described were reviewed and approved by the regional council of Halle (Saale), Germany (Landesverwaltungsamt Sachsen-Anhalt, AZ 42502-2-1258 MLU). Animals were maintained in accordance with the Guide for the Care and Use of Laboratory Animals (Institute of Laboratory Animal Research, 2011).

3.1.1 Laboratory mice and experimental set-up

Inbred C57BL/6 mice (substrain N; Charles River, Sulzfeld, Germany) were used for the investigations. Both sexes were born and raised at the local animal housing facility under standard conditions (21 °C, 45-60 % humidity, group housing at max. 5 adult animals per cage, 12-h circadian light rhythm [lights on from 7 am – 7 pm]). They were provided *ad libitum* access to sterile water and food (maintenance diet for mice; Altromin, Lage, Germany) and assessed regarding state of health and weight gain on regular basis.

Newborn C57BL/6 offspring of at least two simultaneous litters were randomly assigned to interventional (50 % or 75 % FiO₂) and control (20,9 % FiO₂) groups at maximum six neonates per mother/foster mouse.

Three experimental study groups were created to examine the intracellular effects of oxygen treatment onto lung tissue at different ages (Figure 1, **A - C**). In a fourth group, effects of oxygen treatment in early life on later voluntary physical activity was examined (Figure 1, **D**). In group **A**, newborn or infant mice respectively were exposed to moderate or severe hyperoxia for different short amounts of time (10, 30, 60 or 120 min). Animals in group **B** received continuous long-term oxygen treatment for a total of 14 d. Group **C** mice were raised in hyperoxic conditions until infancy (d 14) and subsequently placed to normoxia for a period of 46 days. Group **D** mice were raised similar to group **C**, and after reaching required maturity at about 30 d of age, individually placed to cages equipped with running wheels for analysis of physical activity, as well as nutrition monitoring (see chapter 3.1.4).

Mice were sacrificed and prepared for lung tissue analyses of cellular protein content, free ROS formation and the expression of antioxidant defence systems at given time points (Figure 3).

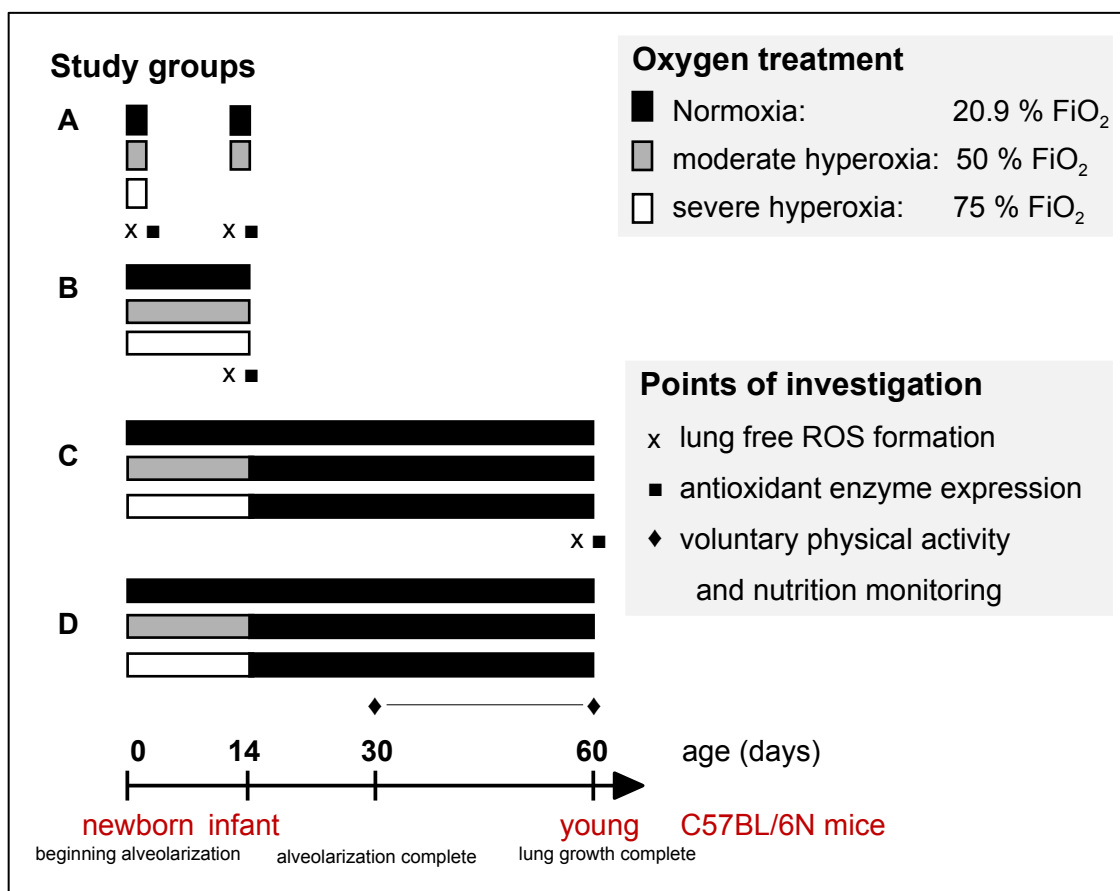


Figure 3: Study set-up for hyperoxia trial

Mice of different ages were assessed for effects of postnatal oxygen treatment. Group **A**: newborn or infant mice's lungs were prepared for investigation directly after short-term treatment. Group **B**: Infant mice's lungs were prepared for investigation after continuous long-term treatment. Group **C**: After long-term treatment, mice were raised in normoxia until lungs were fully developed and prepared for investigation at young age. Group **D**: After long-term treatment and placement in normoxia, voluntary physical activity was measured from age 30 - 60 d. Dissected lungs were analysed for residual formation of free ROS and expression of selected antioxidant enzymes. Lung development is dependent on the age and generally completed by age 60 d.

3.1.2 Oxygen treatment

Study mice randomly assigned to the interventional groups were postnatally placed in a self-constructed airtight polycarbonate chamber, fitting four standard mouse cages (265 x 205 x 140 mm; Bioscape, Emmendingen, Germany). The former is provided with a computerized adjustable gas mixture inflow control system (Aera FC-R7800; Hitachi Metals, Oboke, Japan) (Figure 2). One mother/foster mouse fed up to 6 offspring in a standard polycarbonate cage. The mother/foster mouse of an oxygen treatment group was exchanged with the equivalent mother/foster mouse of a corresponding normoxic control group on daily basis to avoid maternal effects. In case of absence of appropriate increase in body weight, a third foster mouse was included into rotation to feed the litters. This reduced the time spent in hyperoxic conditions for each mother/foster mouse. Previous investigations had shown a weight reduction of

dams in hyperoxic surrounding and hereby induced growth restriction of offspring [30]. Mice were raised under accordant conditions until d 14 of life, subsequently placed to normoxic conditions for final weaning and growth to a minimum weight of 10 g until approximately d 30 of life. At that point, lung alveolarization is known to be completed and mice are ready for separation from mothers.

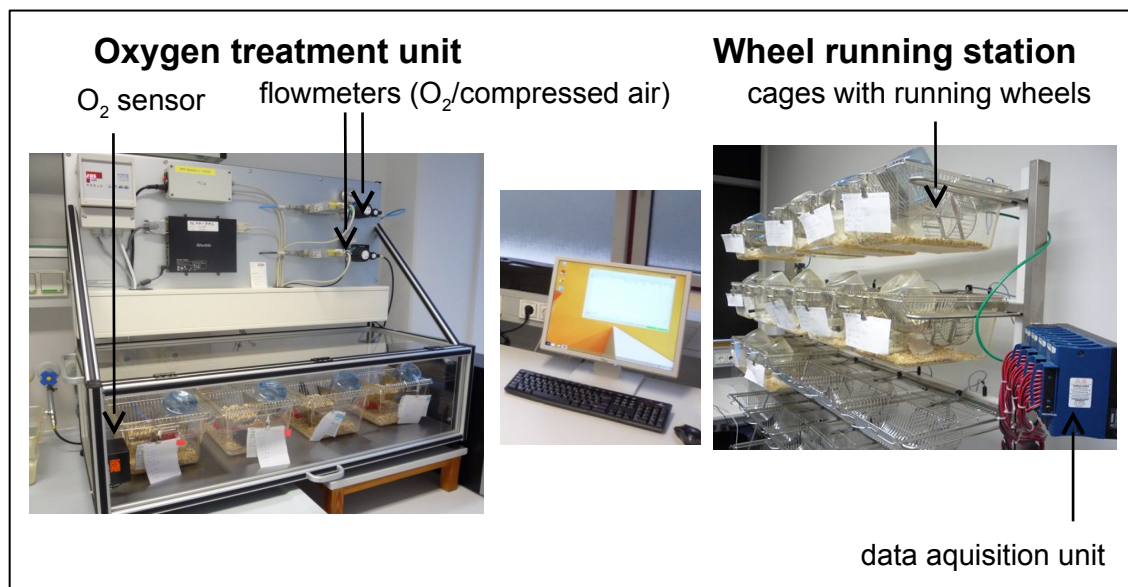


Figure 4: Self-constructed oxygen treatment unit and wheel running station

The polycarbonate chamber (left) fits four standard mouse cages and is connected to a computerized gas inflow regulation system. A built-in oxygen sensor controls the resulting FiO_2 inside the chamber. Cages provided with running wheels (right), as well as individual movement sensors are stored in standard cage racks and connected to the data acquisition unit. A constantly operating computer (centre) gathers information and sends commands through appropriate software.

3.1.3 Recording of voluntary physical activity

After reaching the required maturity, mice were selected for assessment of running wheel activity. Running wheel behaviour has been found to occur even in wild mice in their natural habitat [61], and thereby proved to be an appropriate measure for voluntary physical activity. Preliminary studies have found intersexual differences in voluntary running wheel performance, referring to daily running distance, median velocity and time of breaks in C57BL/6 laboratory mice in favour of the female sex [62]. To enhance possible outcomes in the mentioned parameters and to achieve best comparable results, only female mice were included into this investigation. Animals were placed individually in standard polycarbonate cages (Figure 2), equipped with self-constructed aluminium running wheel systems (115 mm diameter, 50 mm width, 10 mm distance between the bars) connected to a data acquisition unit (Lehnic and Simm, 2010). With the use of permanent magnets connected to the fixed cage as well

as the wheel bars, the rotational movements were tracked as pulses and translated into data by a Compact FieldPoint system (cFP-1804; National Instruments, Austin, TX, USA). These raw data were provided to a constantly operating computer via an internal network. Here they were collected and saved, as well as supplied with minute-by-minute time stamps through installed LabVIEW 8.0 software (National Instruments). Ongoing measurements could be visualized for supervision via graphs for each individual regarding running activity and correct data transmission. Mean group values were generated using timed daily averages of individuals within 24 hours (7 am to 6:59 am the following day, beginning with the inactivity cycle of rodents). In order to gain homogeneously comparable results, data were thereafter analysed between d 37 to d 57 of life of mice (d 7 and 27 of running wheel period) and given as mean value \pm standard error.

3.1.4 Monitoring of nutrition

Before individual placement to single housing at d 30, provided sterile water and standard food were weighed. At time of dissection at d 60 of life, the balance to remaining food and water was calculated and recorded as the individual consumption, divided by days of assessment. Throughout the measurement period, mice had *ad libitum* access to nutrition.

3.1.5 Dissection and sample preservation

Mice at 0 and 14 d of age (study groups **A** + **B**) were to be sacrificed via cervical dislocation through authorized personnel only and subsequently dissected for sample preparation with anatomical instruments. Complete lungs were extracted using dissecting scissors and organ forceps and rinsed in PBS (standardized tablets for dissolution in distilled water, Gibco, Thermo Fisher Scientific, Waltham, USA) solution. Lung lobes were shortly dried on cellulose paper and immediately snap frozen in liquid nitrogen within cold-proof tubes (Eppendorf, Hamburg, Germany).

Mice at 60 d of age (study group **C**) were initially anaesthetized with a prepared mixture of 13 mg per kg bodyweight xylazine (Rompun®, Bayer AG, Leverkusen, Germany) and 65 mg per kg bodyweight ketamine (Ketamin 10 %, WDT, Garbsen, Germany) in 0,9 % NaCl (Merck Millipore, Darmstadt, Germany). The solution was injected intraperitoneally via a 1 ml syringe (B. Braun, Melsungen, Germany). At sufficient narcosis, mice were placed on a self-constructed silicon preparation plate and dissected. A protocol was followed kindly suggested by Prof. Dr. J. Schittny from

University of Bern, Switzerland: The abdominal cavity was opened by a transverse epigastric cut using small surgical scissors. A 10 % heparin (RotexMedica, Trittau, Germany) in PBS solution was injected intracardially via a 1 ml syringe (B. Braun) for systemic anticoagulation. Cervical fasciae were opened and the trachea dissected, where a double cotton string ligature was loosely placed. A 22 Gauge venous catheter (B. Braun) was proximally inserted into the trachea through a small transverse intercartilaginous incision and secured airtight by closure of the ligatures. After perforation of the diaphragm the airways of hereby collapsed lungs were irrigated with 3 x 0.3 ml PBS solution for extraction of bronchoalveolar lavage (BAL). Fluid was collected in a 1 ml reaction tube (Eppendorf) on ice and used for investigations not regarded in this study. The ventral thoracic wall was removed and the large abdominal vessels – aorta and vena cava inferior – cut in fatal approach. After removal of excess blood, as well as heart and thymus gland the right lung was segregated at bronchial level with an additional cotton string ligature. A 20 cm column of 10 % formaldehyde (Merck Millipore) in PBS was installed over the left lung via the tracheal catheter for consistent expansion over 10 min. Subsequently, the four lobes of the right lung were rinsed in PBS and packed separately. Three of them were immediately snap frozen in liquid nitrogen and stored at -80 °C for investigations on reactive oxygen species (ROS), as well as protein quantifications (Figure 3). The fourth lobe was thoroughly dried on cellulose, placed in a previously scaled tube and weighed for determination of partial lung-to-body weight. After drying over 24 hours using Thermomixer comfort (Eppendorf), the assessment of wet-to-dry weight ratio as indicator for lung tissue oedema was performed. Due to this economised dissection technique, no full-lung-to-body-weight ratio could be calculated for mice at 60 days of age. The left lung was placed in 10 ml 4 % formaldehyde in PBS, incubated rotating for 36 hours, subsequently transferred to 70 % ethanol (Sigma Aldrich, St. Louis, USA) and stored at 4 °C until paraffin embedding. Histological investigations were not performed within this study.

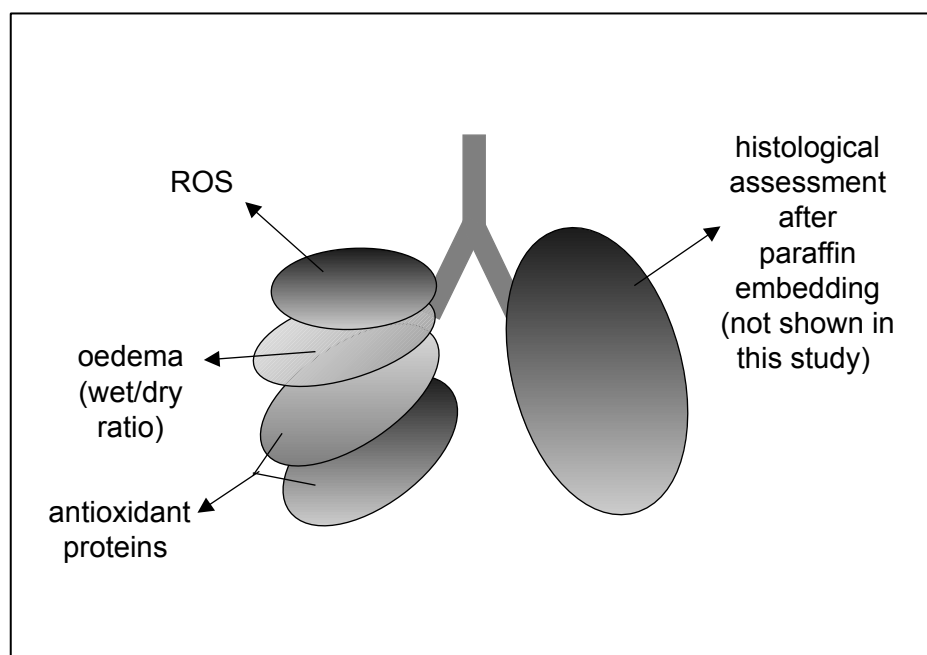


Figure 5: Sample preparation of mouse lung lobes

Anatomical presentation. Left lung lobe was prepared for histological investigations (not presented in this study). Right lung lobes were partly snap frozen for biochemical analysis of free ROS formation and expression of antioxidant enzyme systems. One lobe was scaled and dried for assessment of wet-to-dry weight ratio as indicator for tissue oedema.

3.2 Biochemical methods

If not stated otherwise, chemicals were obtained from the companies Serva, Merck Millipore, Biomol or Sigma-Aldrich.

3.2.1 Sample preparation

(a) For ROS analysis and protein quantification a protocol modified according to Frezza et al. [63] was used for cellular lysis (Figure 6). Deep-frozen lung tissue (see 3.1.5) was weighed on a precision scale (KERN, Balingen, Germany) and placed in 1.5 ml reaction tubes (Eppendorf) on ice for slow defrosting. 5 μ l ice-cold saponin-based lysis buffer (see recipe below) per 1 mg lung tissue was added and tissue homogenised on ice with electrical pestle (Pellet Pestle®, DWK Life Sciences, Wertheim, Germany). The buffer contained Saponine as mild detergent for preservation of mitochondrial membranes, as well as Deferoxamine (DFO) as Fe^{3+} chelator. After incubation on ice for 30 min and repeated short homogenisation samples were centrifuged for 10 min at 300 g and 4 °C (Heraeus Biofuge fresco; Thermo Fisher Scientific) to remove nuclei, attached cytoskeleton and connective fibres. The Supernatant was centrifuged again

for 10 min at 2 500 g and 4 °C in order to isolate a mitochondria (mt-) enriched cellular fraction. The resulting supernatant contained the mt-reduced cytoplasmic cellular fraction and was stored on ice. The pellet was washed with PBS solution, again centrifuged for 10 min at 2 500 g and 4 °C and resuspended in 50 µl saponin lysis buffer for analysis.

(b) For antioxidant enzyme analysis a total protein sample was prepared. Weighed and slowly defrosted lung samples were placed in 1.5 ml reaction tubes and 3 µl SDS-based lysis buffer (see recipe below) added per 1 mg lung tissue. Samples were homogenised on ice using the electrical pestle. After incubation on ice for 15 min and repeated short homogenisation additional 20 µl SDS lysis buffer per 10 mg lung tissue were added and samples again incubated for 15 min on ice. DNA digestion was performed with 1 µl Benzonase® (Sigma Aldrich) for 10 min at 37 °C. Lysates were centrifuged for 10 min at 16 000 g and 4 °C and supernatant transferred to a fresh reaction tube.

Saponin lysis buffer

120 mg HEPES
300 mg KCl
200 µl Na₂-EDTA
500 µl EGTA
200 µl 4 mM DTT
400 µl protease inhibitor cocktail
4.3 g sucrose
25 µl Saponin
50 µM DFO

SDS lysis buffer

400 µl 1 M Tris, pH 7,0
2 ml 10 % SDS
100 µl protease inhibitor cocktail
100 µl 10 µM okadaic acid
100 µl 100 mM sodium vanadate
ad 10 ml H₂O bidest.

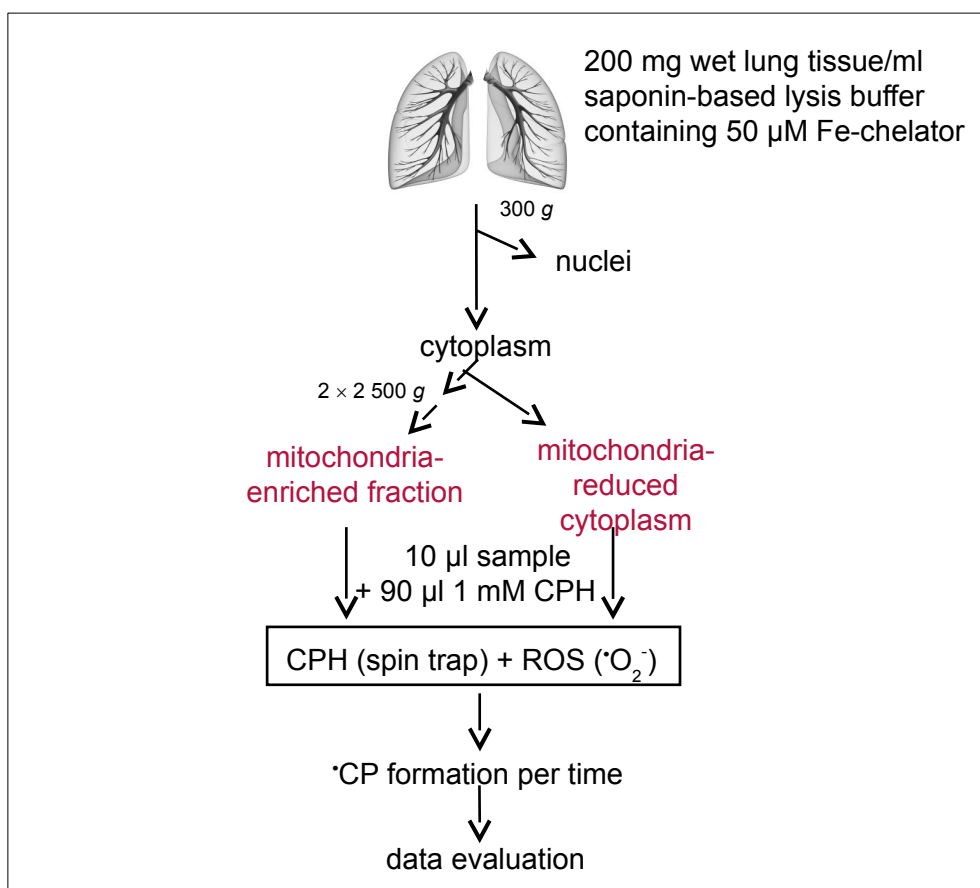


Figure 6: Protein sample preparation in cellular fractions for free ROS analysis (a)

Snap frozen lung tissue was mixed with appropriate amount of saponin lysis buffer and mechanically homogenized. After incubation triple centrifugation was performed to first remove nuclei and then isolate a mitochondria-enriched fraction from mt-reduced cytoplasm. CPH spin trap was added to samples for reaction with free ROS. Thus induced $\cdot\text{CP}$ formation was detected by EPR spectroscopy.

3.2.2 Electron paramagnetic resonance (EPR) spectroscopy

The amount of free ROS molecules produced in lung tissue was detected by the use of electron paramagnetic resonance (EPR) method. A measurement protocol developed in modification of a publication by Adam et al. in 2010 [60] was applied.

Protein samples prepared in chapter 3.2.1 (a) took 1 h 30 min from defrosting until start of the EPR measurement. Stop watches were used for equal time adjustment. 10 μl of each tissue sample were pipetted into a 1,5 ml reaction tube and 90 μl of EPR reagent added (see Figure 6). The latter consisted of aliquots of lyophilised 100 mM CPH (1-hydroxy-3-carboxy-pyrrolidine) (Noxygen Science Transfer and Diagnostics GmbH, Elzach, Germany) dissolved in H_2O bidest. After short blending (Vortex-Genie 2; Scientific Industries, Bohemia, USA), samples were immediately raised into 50 μl glass

capillaries (Brand, Wertheim, Germany), sealed and loaded into the EPR spectrometer (Mini Scope MS100; Magnettech, Berlin, Germany) under adjusted timing. The following device settings were applied: center field 3,368 G, sweep width 100 G, sweep time 60 s, modulation amplitude 1000 mG, receiver gain 50, and power attenuation 6 db. From the start of EPR measurements samples were kept at stable room temperatures (21-25 °C). The detected resonance levels were transmitted to a computerized program and evaluated, using the amplitudes of the low-field line per threefold measurements taken per time point of investigation. Measures were taken over a period of 1 h per sample in 10 min- intervals and amplitude values transferred for determination of linear gain value using Microsoft Excel software (Microsoft Corporation, Redmond, USA). Normalisation of gain to total cellular protein content per each sample was calculated.

3.2.3 Protein quantification

BCA (bicinchoninic acid) method was used to quantify proteins in samples prepared in chapter 3.2.1 **(a)** using the Pierce™ BCA Protein Assay Kit (Thermo Fisher Scientific) and included BSA standard. The procedure was performed as fourfold determination according to manufacturer's instructions in 96-well microtitre plates. Photometric evaluation at 562 nm detection wavelength was conducted using the microtitre Infinite M1000 Reader (Tecan, Männedorf, Switzerland).

3.2.4 SDS polyacrylamide gel electrophoresis (SDS-PAGE) and immunoblot detection

SDS gel electrophoresis was used for separation of proteins in samples prepared in chapter 3.2.1 **(b)**. Polyacrylamide gels consisted of 5 % stacking gel for sample concentration and 15 % running gel for sample separation (see all recipes below). They were loaded into an electrophoresis chamber (Bio-Rad Laboratories, Hercules, USA) and filled with running buffer. Samples containing a defined amount of protein were mixed with sample buffer, incubated at 95 °C for 5 min (Mastercycler gradient; Eppendorf) and then loaded onto the polyacrylamide gel. PageRuler™ Plus prestained protein ladder (Thermo Fisher Scientific) was used as protein molecular weight standard. Voltage was applied to the electrophoresis chamber at 90 V over 175 min on ice for slow and accurate separation of proteins.

Stacking gel (5 %)

520 μ l 40 % Acrylamide/ Bisacrylamide
 500 μ l 1.5 M Tris-HCl, pH 6.8
 2.9 ml H₂O bidest.
 40 μ l 10 % SDS
 25 μ l 10 % APS
 5 μ l TEMED

Running gel (15 %)

2.25 ml 40 % Acrylamide/ Bisacrylamide
 2.25 ml 1.0 M Tris-HCl, pH 8.8
 1.4 ml H₂O bidest.
 60 μ l 10 % SDS
 50 μ l 10 % APS
 5 μ l TEMED

Sample buffer (Sigma Aldrich)

250 mM Tris HCl, pH 6.8
 4 % SDS
 20 % glycerine
 40 mM DTT
 2 mM Na₂-EDTA
 10 ml H₂O bidest.
 0.01 % bromphenolblue

Running buffer

0.25 M Tris, pH 8.8
 1.92 M glycine
 0.1 % SDS

After electrophoresis proteins were blotted onto 0.2 μ m pore size Nitrocellulose Blotting Membrane (GE Healthcare Life Sciences, Little Chalfont, UK) using the Trans-Blot Turbo Transfer System (Bio-Rad Laboratories) and associated special transfer buffer. The procedure was performed according to manufacturer's instructions and a preset blotting program run according to favoured protein sizes. Adequate protein loading was controlled and quantified using amidoblack (AB) staining. Membranes were incubated with amidoblack (AB) solution (Bio-Rad Laboratories) at room temperature for about 1 min, followed by thorough rinsing with tap water. Digital photos were taken with LAS-3000 Imager (Fujifilm, Tokyo, Japan). Then, membranes were blocked with 5 % BSA in PBS-T (PBS solution with 0.1 % Tween added) to avoid unspecific protein binding.

Qualitative and quantitative exploration of antioxidant enzymes of interest was conducted using immunofluorescence detection. Targeted polyclonal primary antibodies were used, followed by secondary antibodies coupled with horseradish peroxidase. The latter is known to enzymatically convert added Luminol Reagent (Santa Cruz Biotechnology, Dallas, USA) into a chemiluminescent product, that can be optically detected by the LAS-3000 Imager. Blotting membranes were incubated at 4 °C over night with primary antibodies according to manufacturer's instructions at the following dilutions:

- CuZnSOD (abcam plc., Cambridge, UK; ab13498) 1 : 1 000
- MnSOD (Rockland Inc., Limerick, USA; 600-401-G13) 1 : 2 000
- catalase (abcam plc., Cambridge, UK; ab15834) 1 : 2 000
- PEX 14 (abcam plc., Cambridge, UK; ab112942) 1 : 1 000
- GAPDH (abcam plc., Cambridge, UK; ab9485) 1 : 2 000

After threefold washing of the membranes in PBS-T, the respective secondary anti-rabbit immunoglobulin antibody (Jackson ImmunoResearch, West Grove, USA) was incubated for 1 h at room temperature in a dilution of 1 : 20 000 in PBS. Membranes were again washed threefold in PBS-T and subjected to luminescence detection upon adding of Luminol Reagent according to manufacturer's instructions in the LAS-3000 Imager. Evaluation of signal intensity was performed using AIDA Image Analysis software (Elysia-Raytest, Straubenhardt, Germany). Protein levels detected by respective antibodies were normalised per protein load assessed via AB staining.

3.3 Statistics

Visualisation and statistical analysis of data was performed using the SigmaPlot 10.0 and SigmaStat 3.5 software (Systat Software Inc., San Jose, USA). Student's t-test (comparison of two groups) and ANOVA with Holm-Sidak method (parametric data) or ANOVA on Ranks followed by Dunn's method (non-parametric data) were performed for assessment of statistical relevance. If not indicated otherwise, data are given as mean \pm standard deviation or standard error. Area under curve (AUC) calculations were performed using Microsoft Excel software (Microsoft Corporation) for assessment of total running distance. Data of the respective treatment groups were tested for significant differences in mean values using the Student's t-test and ANOVA as indicated. P-values < 0.05 indicate significant differences.

4. Results

Three study groups (**A-C**) were generated to assess the effect of moderate and severe hyperoxia in early childhood on the lung tissue of mice (see Figure 12). For the latter, intracellular formation rate of free ROS and expression of selected antioxidant defence enzymes were analysed. In group **A** the immediate effect of oxygen administered to newborn or infant mice was studied, whereas group **B** mice were analysed for the long-term effect of hyperoxia after 14 days. Group **C** mice were used to outline the long-term consequences of postnatally administered oxygen treatment.

In a fourth study group (**D**) the impact of postnatal oxygen treatment on later voluntary physical activity was tested by use of a running wheel system. Additionally, individual nutrition was monitored in this group to identify potential differences in consumption due to increased activity.

4.1 General data of mouse groups

Study group A: The direct effect of ventilation under moderate or severe hyperoxic conditions for short durations (10, 30, 60, 120 min) on lung tissue of newborn or infant mice was studied in this group. Animals showed appropriate increase in lung weight within each treatment group when compared to newborns (Table 2). Body weight was not equally measured in all individuals and therefore not presented.

Table 2: Study group A: general data of newborn and infant mice treated with short-term hyperoxia (10 - 120 min)

Parameter		newborn			infant	
		N	mH	sH	N	mH
sex male : female	(n)	15 : 18	13 : 12	26 : 7	9 : 9	11 : 13
absolute lung weight	(mg)	44.6±12.8	39.7±7.62	40.7±6.72	89.5±12.0	85.8±15.2

Data are given as mean ± SD; N (normoxia), mH (moderate hyperoxia), sH (severe hyperoxia)

Study group B: After a continuous oxygen exposure for a total of 14 d, the effects on infant mice were studied in this group. A higher body weight of animals in the sH group was present compared to N or mH mice. This could possibly be a side effect of a third foster mouse frequently used in this treatment group. Lung-to-body-weight ratio was equal in all groups (Table 3).

Table 3: Study group B: General data of infant mice treated with long-term hyperoxia

Parameter		N	mH	sH
sex male : female	(n)	21 : 12	11 : 3	8 : 9
body weight	(g)	5.8 ± 1.29	5.3 ± 0.66	7.1 ± 1.28*
full lung-to-body-weight ^a	(%)	1.4 ± 0.26	1.5 ± 0.1	1.4 ± 0.14

Data are given as mean ± SD; ^a complete lung weight was normalized to body weight; * p < 0.001 vs. N or mH (ANOVA with Holm-Sidak method); N (normoxia), mH (moderate hyperoxia), sH (severe hyperoxia)

Study group C: The long-term consequences of oxygen treatment during early infancy were studied in this group, analysing free ROS formation and antioxidant enzyme expression at d 60 of life. Concordant to animals of study group B, mice in the sH group show a higher body weight compared to N or mH group mice. Partial lung-to-body-weight ratio was equal in all groups (Table 4).

Table 4: Study group C: General data of young mice treated with long-term hyperoxia and subsequent normoxia

Parameter		N	mH	sH
sex male : female	(n)	5 : 19	10 : 14	13 : 3
body weight	(g)	16.5 ± 3.3	18.1 ± 2.4	20.45 ± 2.6*
partial lung-to-body-weight ^a	(%)	0.14 ± 0.03	0.13 ± 0.02	0.13 ± 0.02

Data are given as mean ± SD; ^a only one lung lobe was weighed due to methodical reasons (see chapter 3.1.5); * p < 0.001 vs. N and p < 0.05 vs mH (ANOVA with Holm-Sidak method); N (normoxia), mH (moderate hyperoxia), sH (severe hyperoxia)

Study group D: In order to assess the effect of hyperoxic air conditions during infancy on voluntary physical activity and performance later in life, we provided mice with running wheels after reaching childhood at about 30 d of age. Because of sex-dependent differences in the running activity [62], only female animals were included. By the end of the test period at d 60 there were no obvious differences found in general characteristics of mice between the different treatment groups (Table 5). The assessed wet-to-dry lung weight ratio did not indicate the formation of apparent lung oedema due to postnatally administered oxygen treatment.

Table 5: Study group D: General data of young mice provided with running wheels for 30 days

Parameter		N	mH	sH
sex male : female	(n)	0 : 17	0 : 17	0 : 16
body weight	(g)	19.1 ± 2.93	19.0 ± 3.24	18.6 ± 2.66
partial lung- α-to-body-weight ^a	(%)	0.13 ± 0.03	0.12 ± 0.02	0.13 ± 0.02
lung wet-to-dry ratio		8.1 ± 1.47	7.8 ± 1.37	8.5 ± 2.47

Data are given as mean ± SD; ^a only one lung lobe was weighed due to methodical reasons (see chapter 3.1.5); N (normoxia), mH (moderate hyperoxia), sH (severe hyperoxia)

4.1.1 Effect of hyperoxia on running wheel activity and nutrition

Food and water consumption, as well as weight gain were monitored during the running wheel period and showed no significant differences between the treatment groups in the end (Table 6). Parameters of assessment of running wheel activity also did not indicate significant effects related to postnatal oxygen treatment.

Table 6: Nutritional and running wheel parameters of young mice provided with running wheels for 30 days (study group D)

		N	mH	sH
Nutritional parameters^a				
food consumption	(g · d ⁻¹)	4.2 ± 0.45	4.8 ± 1.20	4.4 ± 0.63
water consumption	(g · d ⁻¹)	6.1 ± 1.19	6.5 ± 1.51	6.1 ± 0.77
weight gain in running wheel	(g · 30 d ⁻¹)	5.3 ± 2.14	5.7 ± 2.45	4.6 ± 1.85
Running wheel parameters^b				
total run distance, sum	(km)	143.8 ± 9.49	136.7 ± 8.27	142.8 ± 12.16
mean velocity	(m · min ⁻¹)	21.4 ± 1.10	21.4 ± 0.62	21.2 ± 0.99
breaks > 5 min	(n · d ⁻¹)	60.3 ± 2.32	64.9 ± 2.03	60.2 ± 2.97

^a Data are given as mean ± SD; ^b Data are given as mean ± SE; N (normoxia), mH (moderate hyperoxia), sH (severe hyperoxia)

Distance covered was automatically assessed every minute and given as individual sum of run meters per day. All treatment groups presented with a roughly similar and rather uneven performance of their daily running distance (Figure 7 above), but finally no significant differences could be shown. By the end of investigations, all treatment groups on average presented with a similar total distance run over the observation period of 30 days (Table 6).

Median velocity was assessed in the same manner and given as average speed per minute. All treatment groups showed a steady incline of running velocity over time (Figure 7 center), whereby they seem to delineate a saturation curve. No significant differences could be shown in between the study groups.

Breaks from running were defined as non-recognition of movement in running wheels that exceeded 5 minutes. Data are given as average number of breaks > 5 min per day within the group. The assessment of average number of breaks again showed similar values for all treatment groups (Figure 7 below).

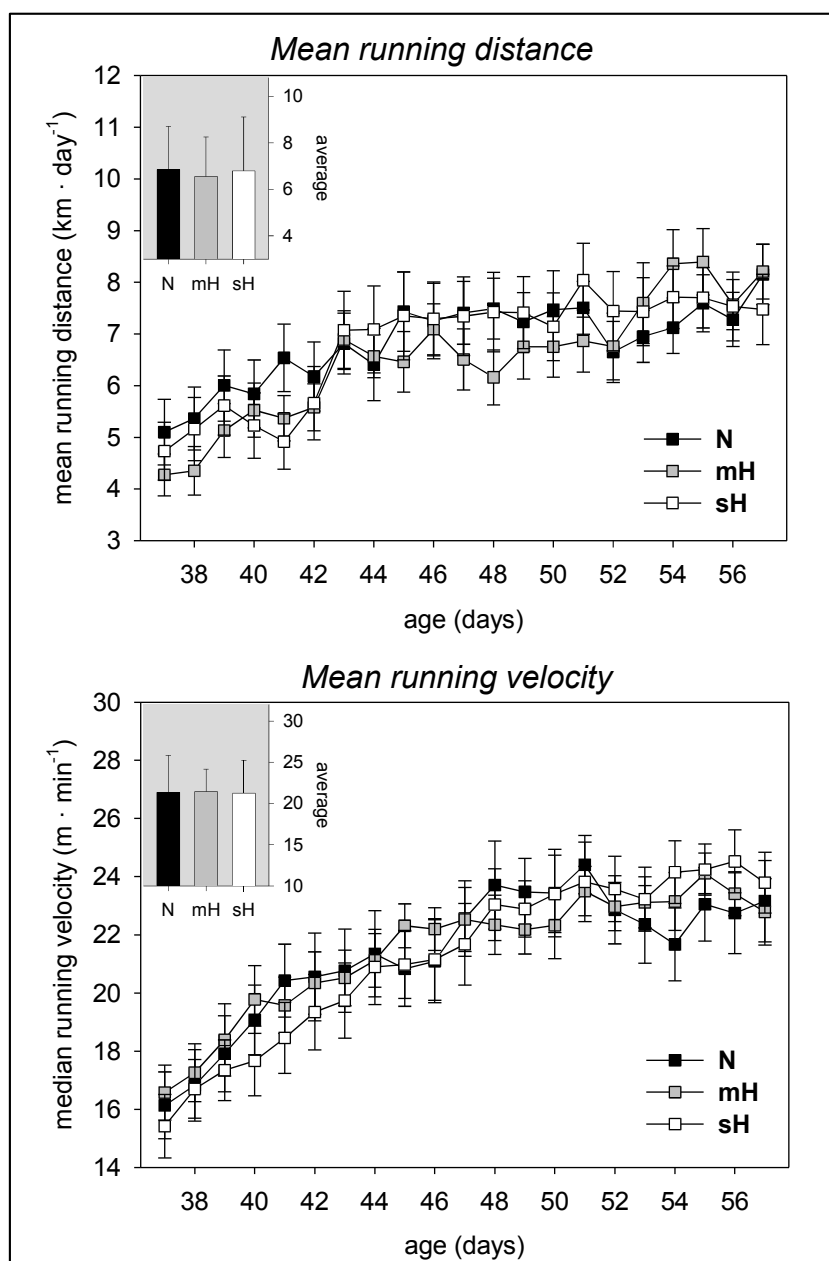


Figure 7: see next page

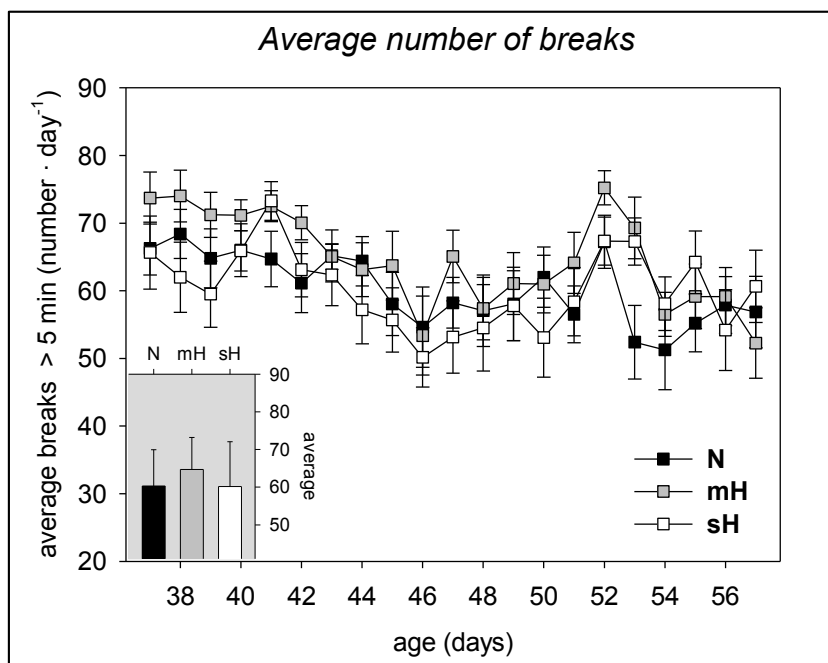


Figure 7: Mean running distance, mean running velocity and average number of breaks per day

Running wheel activity of female mice was constantly monitored and presented for mice 37 – 57 d of age (study group **D**). Daily group averages were charted, bar graphs show group averages over the evaluation period for each parameter. No significant differences could be found between the treatment groups. Data are given as mean \pm SE; N (normoxia), mH (moderate hyperoxia), sH (severe hyperoxia)

4.2 Results of biochemical analyses

After sample preparation in the manner described in chapter 3.2.1, deep-frozen lung tissue was utilized for qualitative and quantitative biochemical analyses.

4.2.1 Influence of age and hyperoxia on cellular protein levels

Lung tissue consists of extra- and intracellular proteins. Since my preparation method used for ROS detection obtained mainly intracellular proteins, I expected age- and potentially treatment-dependent differences in the cellular protein amount per weighed lung tissue.

This expectancy could be verified, as untreated young mice had significantly lower levels of cellular protein per lung tissue weight than untreated newborn and infant mice (Figure 8). Also, the long-term sH ventilation tended to have effects on the proportion of cellular protein to total lung tissue weight in young mice.

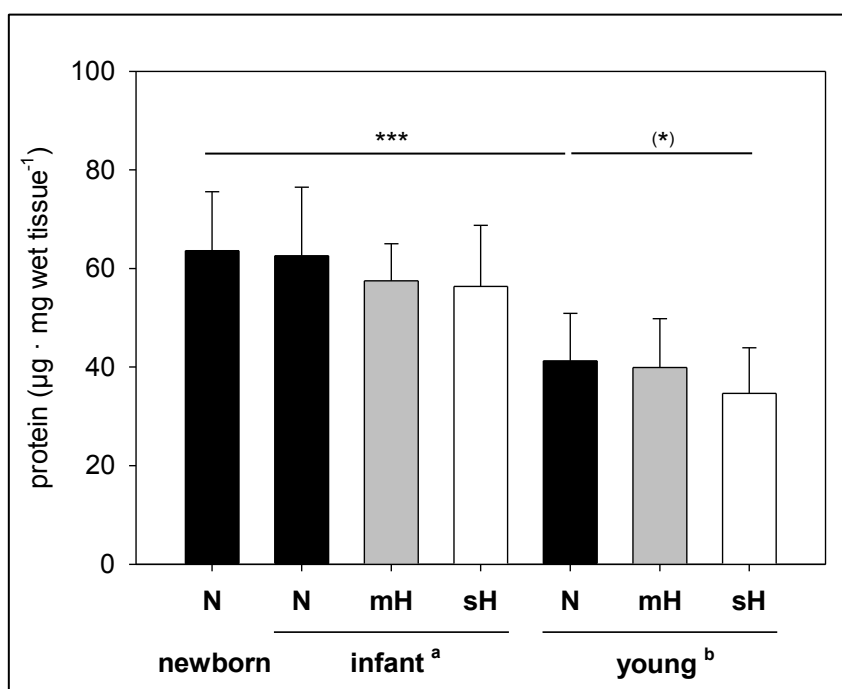


Figure 8: Cellular protein content per lung wet tissue weight

Protein quantification was assessed using SDS-PAGE and immunofluorescence. Data are given as mean \pm SD; *** $p < 0.001$, (*) $p < 0.1$ (ANOVA with Holm-Sidak method); ^a mice after 14 days of treatment with different oxygen concentrations (study group **B**); ^b mice 45 days after 14 days of treatment with different oxygen concentrations (study group **C**); N (normoxia), mH (moderate hyperoxia), sH (severe hyperoxia)

4.2.2 Characterisation of fractionation of cellular compartments

Initially, separate measurements of free ROS in mt-enriched and -free fractions were planned. Therefore, both fractions were checked for their quality via immunoblot procedure using antibodies against cell compartment-specific marker proteins. These were MnSOD for mitochondrial matrix, Catalase for peroxisomal matrix, PEX14 for peroxisomal membranes and GAPDH for cytosol. As demonstrated in Figure 9, the mt-enriched fraction also contained peroxisomes. This was somewhat surprising because peroxisomes are much smaller than mitochondria and should have been separated by the performed differential centrifugation. These findings indicate a possible complex formation of the two organelles. Since the quality of ROS measurements would have been adversely affected by further purification of the mitochondrial fraction, I continued to use this mt-enriched and peroxisome-contaminated fraction for selected measurements.

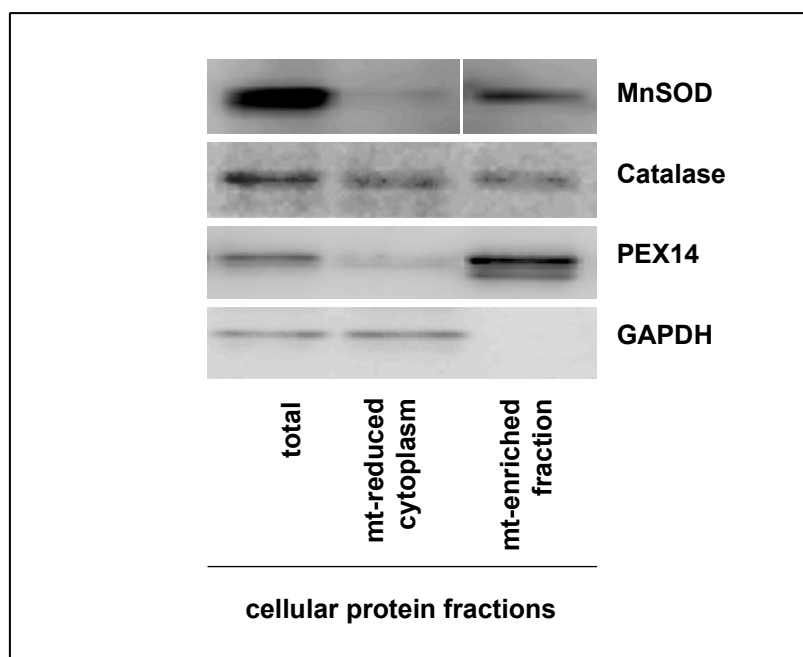


Figure 9: Qualitative protein analysis of cellular fractions

Detection of marker proteins for mitochondria, peroxisomes and cytoplasm in separated cellular fractions using SDS-PAGE and immunofluorescence

The protein level of both the cytoplasmic and mt-enriched fraction was quantified relative to the amount of lung tissue used per sample. As shown in Figure 10, the protein level of the mt-enriched fraction is located between 2.5 - 4 μg protein per mg lung tissue with lowest values for infant mice. The respective protein amount of the mt-reduced cytoplasmic fraction is much higher. Similar to results presented in Figure 8, young mice show significantly lower amounts of mt-reduced (cytoplasmic) protein compared to newborn or infant mice.

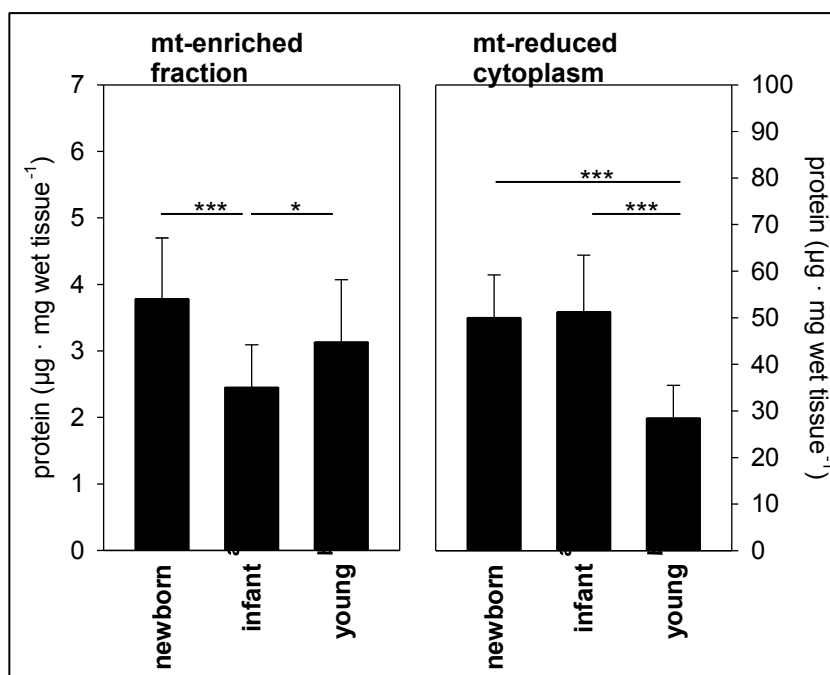


Figure 10: Absolute protein content of cellular fractions isolated from mouse lung tissue depending on age

Protein quantification was assessed using SDS-PAGE and immunofluorescence. Data are given as mean \pm SD; *** $p < 0.001$; * $p < 0.05$ (ANOVA with Holm-Sidak method or ANOVA on Ranks followed by Dunn's method); ^a mice after 14 days of treatment with normoxia (study group **B**); ^b mice 45 days after 14 days of treatment with normoxia (study group **C**)

Measurement of free ROS formation in the mt-enriched and -reduced fractions using the CP-H spin trap revealed quantitative differences in \cdot CP formation between both cellular fractions. This was highly influenced by the normalisation method of choice (see Figure 11). Normalisation per respective protein amount indicated a comparatively high enzymatic free ROS formation in both cellular fractions. Conversely, when normalised to the overall tissue weight, ROS signal intensity was significantly higher in the mt-reduced cytoplasm than in the mt-enriched fraction.

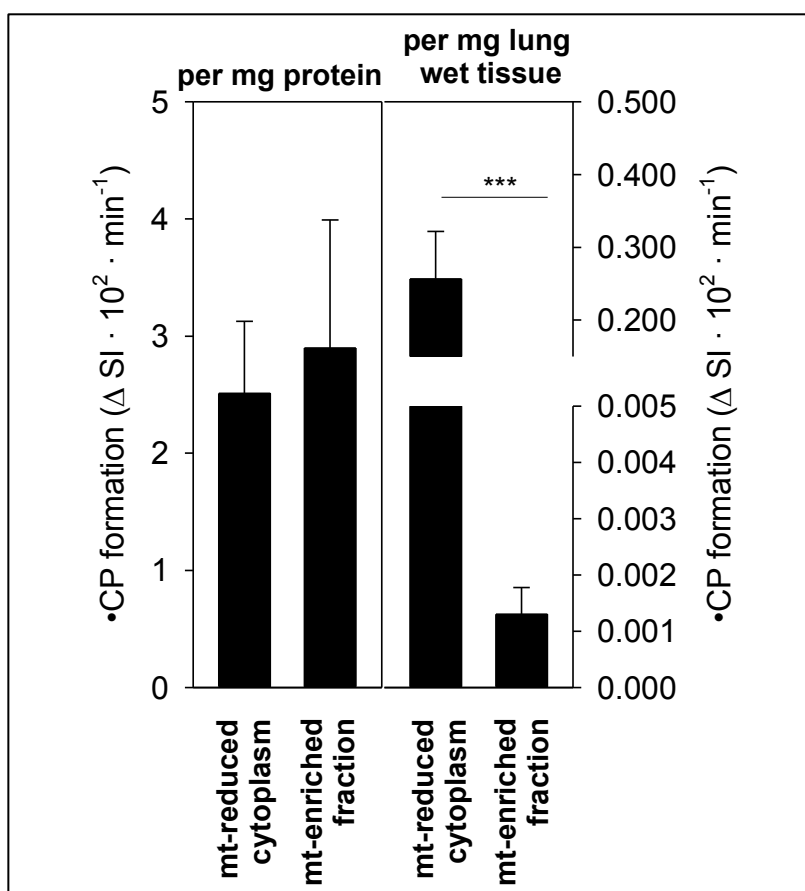


Figure 11: Free ROS formation in cellular fractions per protein or lung wet tissue in untreated infants (study group B)

Normalisation per sample protein content depicts the distribution of intracellular free ROS production. Free ROS formation was assessed by EPR technology using the CP-H spin trap. Data are given as mean \pm SD; *** $p < 0.001$ (Student's t-test)

Considering the prominent age-dependency of the proportion of isolated cellular proteins per lung weight (see Figure 10), ROS data were subsequently normalised per protein amount extracted from the sampled tissue and not per lung tissue weight.

Subsequent fractionated cellular analysis of free ROS formation also revealed a significant effect of age with lowest •CP formation in infant lungs (Figure 12).

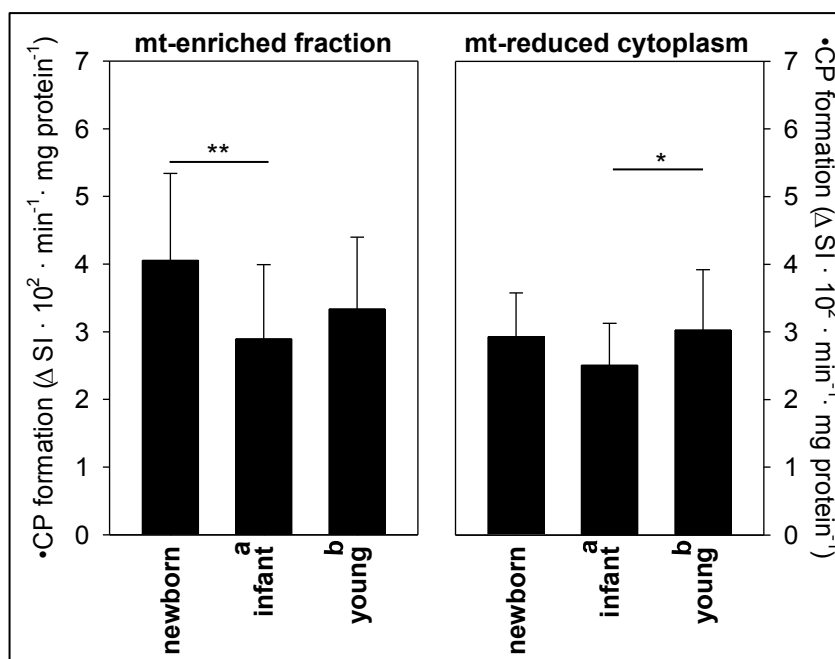


Figure 12: Free ROS formation in cellular fractions per different age groups

Free ROS formation in both cellular compartments of untreated mouse lungs. Free ROS formation was assessed by EPR technology using the CP-H spin trap. Data are given as mean \pm SD; * $p < 0.05$; ** $p < 0.01$ (ANOVA with Holm-Sidak method); ^a mice after 14 days of treatment with normoxia (study group **B**); ^b mice 45 days after 14 days of treatment with normoxia (study group **C**)

4.2.3 Effect of short-term oxygen treatment

The short-term oxygen treatment under moderate hyperoxic conditions was compared between newborn and infant mice regarding free ROS formation in the mt-enriched and -reduced fractions. These analyses indicated that free ROS formation levels in infant mice tend to decrease over time and are lowest after 120 min of moderate hyperoxic ventilation in both fractions (Figure 13). This progressing reduction was less obvious in lung samples of newborn mice, in part due to their higher basal levels of free ROS formation, especially in the mt-enriched fraction (Figure 13).

In addition to moderate hyperoxia, short-term oxygen treatment inducing severe hyperoxia was administered to newborn mice only. Compared to mH conditions, severe hyperoxic treatment did not significantly affect the time-dependent formation of free ROS in lungs of newborns (Figure 14).

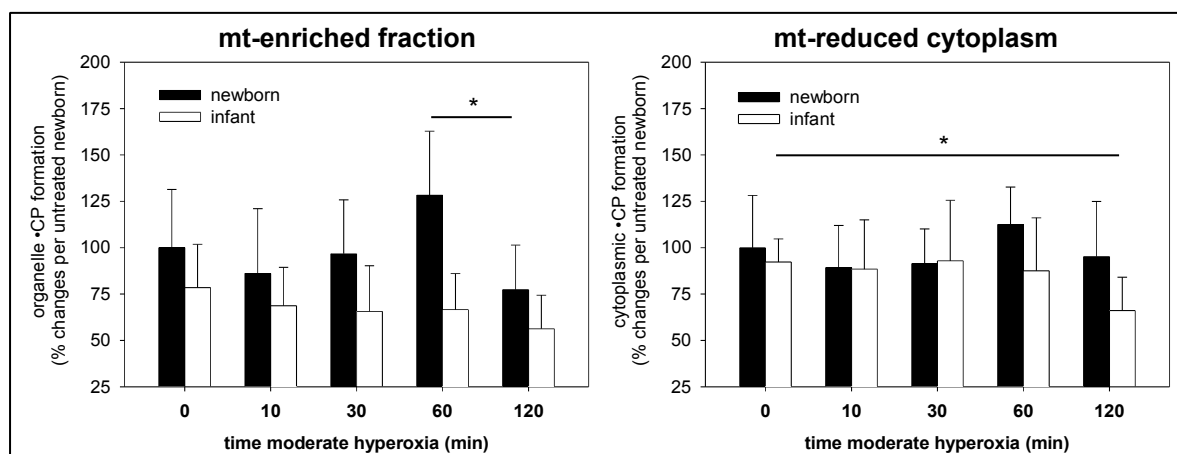


Figure 13: Free ROS formation in mt-enriched organelle fraction and mt-reduced cytoplasm after short-term mH ventilation in newborn and infant mice per untreated newborn (study group A)

Free ROS formation was assessed by EPR technology using the CP-H spin trap. Data are given as mean \pm SD; * $p < 0.05$ (Student's t-test of isolated groups)

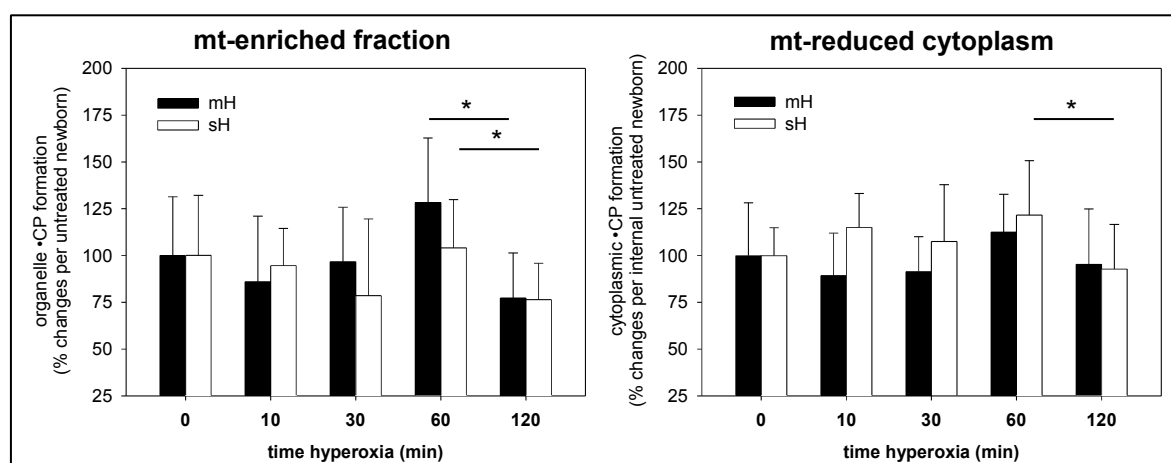


Figure 14: Free ROS formation in mt-enriched organelle fraction and mt-reduced cytoplasm after short-term mH and sH ventilation in newborn mice per untreated newborn (study group A)

Free ROS formation was assessed by EPR technology using the CP-H spin trap. Data are given as mean \pm SD; * $p < 0.05$ (Student's t-test of isolated groups)

In summary, short-term hyperoxia did not significantly alter the free ROS formation in lungs of newborn and infant mice immediately after treatment. However, after 120 min of hyperoxia treatment the intrinsic formation of free ROS in mouse lung tissues of newborn and, even more pronounced, infant mice appears to be minimised (Figures 13, 14).

4.2.4 Effect of age and long-term oxygen treatment on free ROS formation

Parallel measurements of free ROS formation in both the mt-enriched and mt-reduced fractions did not show a differential effect (see Figures 13 and 14). Also, the mt-enriched organelle fraction was contaminated with peroxisomes (Figure 9) and the main free ROS production was shown to take place in the mt-reduced cytoplasm (Figure 11). For the given reasons, a total cytoplasmic protein fraction was analysed for subsequent investigations and mitochondria isolation has been renounced. Therefore, sample preparation was completed after the first step of centrifugation (see chapter 3.2.1 (a)).

Figure 15 summarises the data resulting from free ROS detection using the CP-H spin trap in non-mt-reduced cytoplasm lung samples of mice from study groups **A**, **B** and **C**.

This summary indicates no significant difference in the basal lung free ROS formation between newborn, infant and young mice. Moderate long-term hyperoxia after birth causes an increase of lung free ROS in young mice (45 days after treatment) but a decrease in infant mice (directly after treatment). Surprisingly, long-term severe hyperoxia after birth had no significant effect later in life (Figure 15).

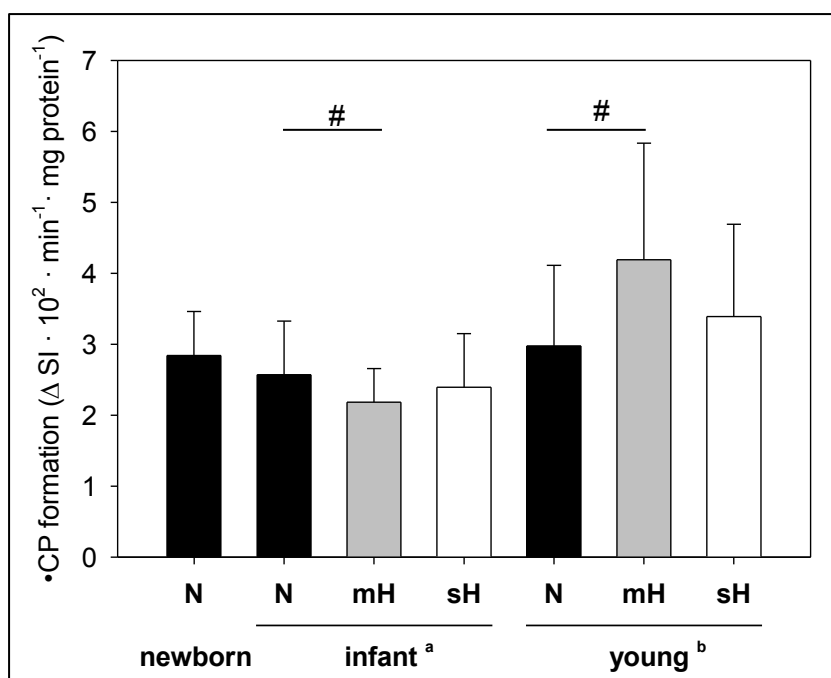


Figure 15: Free ROS formation in mouse lung tissue depending on age and long-term oxygen treatment

Free ROS formation was assessed by EPR technology using the CP-H spin trap. Data are given as mean \pm SD; # $p < 0.05$ comparison dependent on treatment; ^a mice after 14 days of treatment with different oxygen concentrations (study group **B**); ^b mice 45 days after 14 days of treatment with different oxygen concentrations (study group **C**)

4.2.5 Effect of age and long-term oxygen treatment on antioxidant systems

The expression of selected enzymatic systems involved in antioxidant defence was studied depending on age of mice and level of postnatal long-term oxygen treatment. Total lung tissue lysates were analysed for copper zinc superoxide dismutase (CuZnSOD), manganese superoxide dismutase (MnSOD) and catalase. Again, all data of mice (study groups **A**, **B** and **C**) were presented together for a better overview (Figure 16).

My analysis of the representative antioxidant defence enzymes showed a detectable amount of CuZnSOD, MnSOD and catalase in lung tissue directly after birth. Age-dependent analysis then showed a quantitative increase of all three enzymes with an early increase in catalase and a late increase in both SODs (Figure 16). A significant influence of the severity of postnatal long-term hyperoxia on the respective enzyme expression could only be found in lungs of infant mice. Precisely, MnSOD expression was increased directly after long-term severe hyperoxia and catalase expression was increased after long-term moderate hyperoxia. Young mice did not show significantly different expression levels of the selected enzymes in response to postnatal hyperoxia.

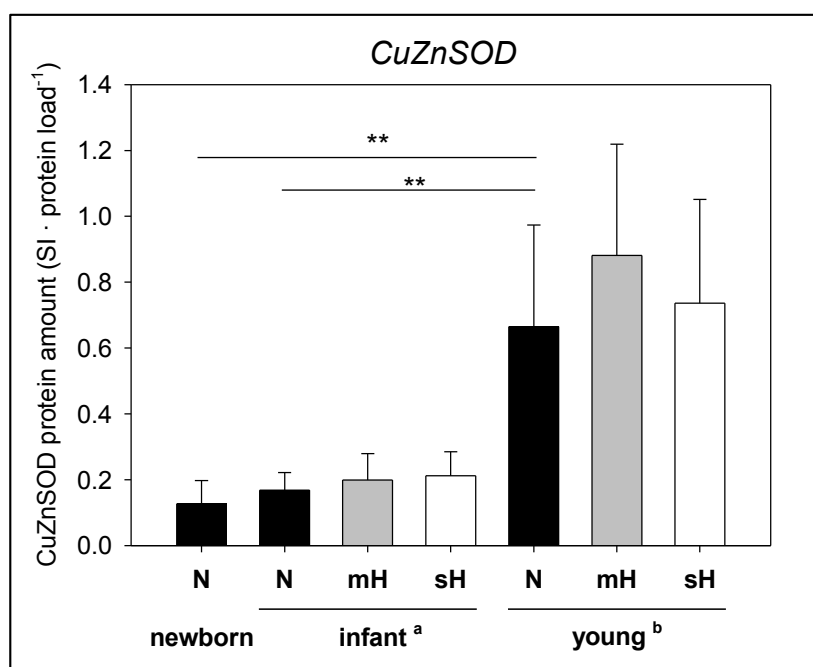


Figure 16: see next page

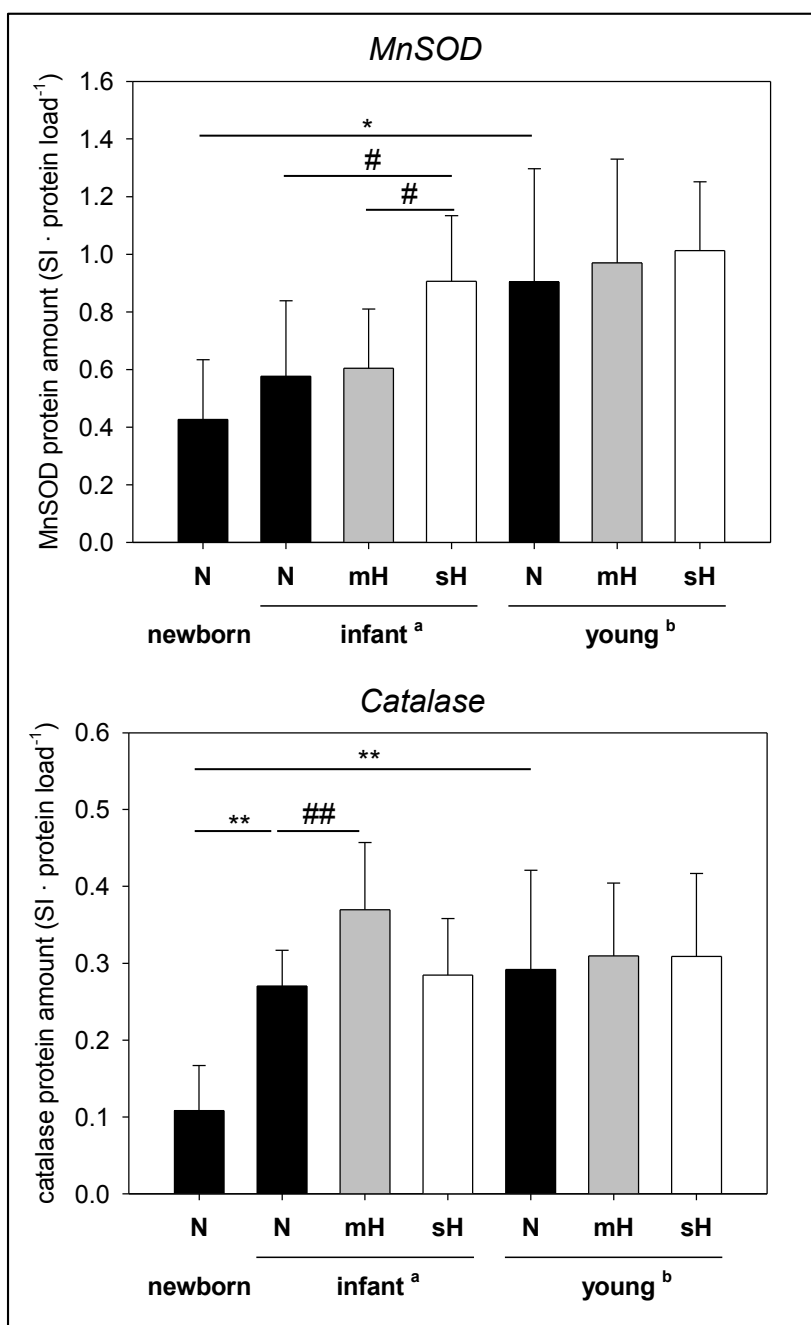


Figure 16: Protein expression of selected antioxidant defence enzymes dependent on age and long-term oxygen treatment of mice for CuZnSOD, MnSOD and catalase

Protein quantification was assessed using SDS-PAGE and immunofluorescence. Data are given as mean \pm SD; * $p < 0.05$, ** $p < 0.01$, *** $p < 0.001$ comparison dependent on age; # $p < 0.05$, ## $p < 0.01$ comparison dependent on treatment (ANOVA on Ranks, followed by Dunn's method); ^a mice after 14 days of treatment with different oxygen concentrations (study group **B**); ^b mice 45 days after 14 days of treatment with different oxygen concentrations (study group **C**)

5. Discussion

Molecular oxygen has evolved as a very important medication widely used for numerous clinical indications. High pressure mechanical ventilation is already known to cause structural damage to lung tissue [64], but the isolated role of oxygen administration in the process of damage is not well understood yet. Tissue hyperoxia caused by the therapeutic administration of hyperbaric oxygen is known to mediate cellular toxic damage and inflammation (for review [22],[51]). This is assumed to partly emerge from free oxygen radical formation directly resulting from the oxygen plethora in the surrounding air (for review [23]). Scientific focus has been on the assessment of mechanisms reducing the negative effect of hyperoxia on tissue structure. But so far not on the effect of previous hyperoxia on the ongoing intrinsic production of free ROS molecules, which carry an important role within the cellular homeostasis (see chapter 1.4.1). The detection of intracellular free ROS molecules is difficult due to their short half life and the various and potent scavenging and antioxidant mechanisms. Most available tests are indirect *in vitro* or *ex vivo* measurements with complicated protocols [43], therefore analyses on the matter are only few. My assessment only showed changes of intrinsic free ROS production following moderate hyperoxia, as well as an overall unaffected long-term expression of antioxidant enzymes.

5.1 Influence of hyperoxia on free ROS formation and antioxidant enzymes

By use of an indirect ROS measurement method I was able to show no relevant influence of postnatal short- and long-term oxygen treatment onto the intrinsic cellular free ROS formation in mouse lungs (Figures 13 - 15). Only moderate hyperoxia was found to slightly modify intrinsic free ROS formation: I could show a decrease of ROS production rate after 120 minutes of short term treatment in newborns. Long-term treatment under moderate hyperoxia caused diverging effects dependent on the age of treated individuals: free ROS production was slightly reduced directly after 14 days of treatment in infant mice. Adversely, moderate long-term hyperoxia induced a slight increase of intrinsic ROS formation in young mice 45 days after long-term treatment. It has to be taken into consideration here that untreated infant mice generally show a slightly lower base rate of free ROS formation compared to other age groups, which was distributed equally over mt-enriched and -reduced fractions (Figure 12). This indicates no major age- and development-related differences in free ROS formation, considering the change of intracellular protein levels determined by growth-related protein turnover.

Nevertheless, a possible long-term effect of only moderate postnatal hyperoxia onto cellular free ROS formation should be further investigated. In the present setting it was not possible to determine why only moderate and not severe hyperoxia were able to change free ROS formation rates.

According to my results, a change of intrinsic free ROS production can not directly be made responsible for cellular damage resulting from hyperoxic treatment. But as further investigations of my supervisor's research group showed, induced tissue hyperoxia did cause emphysema-like changes in the extracellular spaces later in life [65]. My colleagues performed *ex vivo* measurements of lung function in adult mice at the age of 120 days, as well as histological assessments of lung tissue at 60 days. They showed a reduction in alveoli number, thickening of alveolar walls and augmentation of larger airspaces in adult mice (60 d), as well as an increase in lung compliance in advanced adulthood (120 d) following postnatal oxygen treatment with 75 % FiO₂ (sH group). These changes could not be found, or only in attenuated occurrence, in mice of the mH group and do not correspond with my findings of moderate hyperoxia being the most influential.

Related to the above findings, Datta et al. found structural changes to lung tissue within the first postnatal days of mice treated with induced hyperoxia (75 % FiO₂ was administered over a period of 72 h). These changes included compromised pulmonary alveolarisation, decreased septation and increased distal artery muscularisation - findings which indicate towards compromised postnatal alveolarisation processes. The induced damages showed a significant decrease in severity when oxygen treatment started only from postnatal day 4 compared to day 0 and were able to be attenuated by the simultaneous administration of a mitochondria-targeted antioxidant [29]. This indicates a continuous postnatal decrease in susceptibility of murine lung tissue to induced oxidative stress over time.

As stated in chapter 1.4.3, the postnatal development of antioxidant defence systems is not yet fully understood. Neonates of many species seem to adapt more easily to a hyperoxic environment compared to young and adults [26] (for review [22]). This can be due to their physiologic 'preparedness' against a hyperoxic boost through a higher antioxidant system response (for review [53]). It has been shown that oxygen treatment inducing severe hyperoxia increased expression levels of MnSOD, but not CuZnSOD, in murine lung tissue only when administered directly postnatally, but not after postnatal day 4 [29]. This gives an idea about the fast postnatal maturation of intracellular antioxidant defence enzyme mechanisms and could possibly be an explanation for the sufficient adaptation of neonate and infant individuals.

I could display that mice showed a somewhat physiological change in expression levels of intracellular antioxidant enzymes throughout growth period with overall highest base expression rates at adult age. In detail, base expression rates of the cytoplasmic CuZnSOD and mitochondrial MnSOD increased only at young age, whereas the peroxisomal catalase shows an up-regulated expression already at infant age. Postnatal long-term oxygen treatment did influence the antioxidant enzyme expression rate directly *post interventionem* at infant age, an effect that did not last into adulthood (Figure 16). These findings could only partly explain the effect of hyperoxia on free ROS formation. Up-regulation of catalase expression in infants directly after long-term moderate hyperoxia can possibly be made responsible for the decrease of free ROS formation in this group, but only if the overall lower base rate in infancy was taken out of consideration.

5.2 Influence of hyperoxia on voluntary physical activity

Prematurely born human infants in need of perinatal respiratory support were shown to experience pulmonary impairment later in life, which can be coherent to a decline in exercise capacity [33]. The physical development of mice was not impaired in my investigations, but even showed a beneficial effect in body weight under long-term oxygen therapy inducing severe hyperoxia in infant and young mice (see Tables 3 and 4). Also, mice of all treatment groups seemed to adapt well to the level of physical exercise later in life and showed a homogeneous training effect. There was also no indication for an altered requirement of nutrition for any group during that exercise period.

The voluntary physical activity in mice is generally very high in relation to their body length. My findings of overall unimpaired physical development of mice as well as their voluntary running performance show no major negative influence of previous postnatal oxygen treatment. These findings are congruent to the human study of Winck et al., who examined previously very-low-birth-weight preterm neonates at school age [34]. They did not find significant changes in lung function and physical development compared to a control group of previously normal birth weight neonates. Nevertheless, it has to be considered that the general lung reserve is very high and in neither of the named experiments the full lung functional capacity was exploited, which would be achieved by forced training upon exhaustion. This has been executed by van Haaften et al., who subjected infant rats previously raised under very severe hyperoxic conditions (95 % FiO₂ for 14 days) to subsequent forced treadmill training upon exhaustion [35]. Under these extreme treatment and workout conditions, they were able to show a significant decrease in exercise capacity of rats exposed to hyperoxia compared to nor-

moxia. Transferring this to the human situation, the examiner would have to force young children who have developed severe structural pulmonary changes due to prematurity and intense perinatal oxygen treatment to forced competitive sports. This induces the assumption that the structural tissue damage found in adult mice after postnatal moderate or severe oxygen treatment [65] is not severe enough to compromise the functional lung reserve during moderate physical exercise, but only when exploiting the full lung capacity.

5.3 Technical aspects of murine hyperoxia trials

The method of a mouse model is adequate, but in order to portray an unphysiologic and even life threatening state such as the underdeveloped lung in a severely preterm infant, it lacks precision. For the increase of statistical relevance, the number of animals per examination group should be increased in subsequent trials. Possibly, the tendency found can be turned into significant results.

The applied oxygen levels in our study were representative for average oxygen levels administered in early postnatal care, but could not be administered according to current therapeutic guidelines and clinical standards. These dictate a titrated oxygen administration in adaptation to the patients' underlying condition and current clinical status measured via peripheral oxygen saturation of the blood (SaO_2), respiratory distress as well as ventilation parameters [66]. This very individual treatment approach limits standardisation in experimental representations. Within the examination groups I found a surprising effect of oxygen application on physical development and growth of the treated mice (Tables 3 – 5), such that animals after induced sH were larger in size. This finding could come under an inadvertent maternal effect, since we rotated the mother/foster mice between N groups and mH or sH groups, respectively. Hence, newborns of the sH group received newly recovered dams from normoxia and thereby possibly better nutrition compared to the control group. As mentioned above, it has been found that hyperbaric oxygen treatment has a more severe effect on adult mice rather than infants showing in growth restriction [30]. Therefore, we have to assume a possible impact of hyperoxia on lactation as well, lasting longer than the short treatment times of a few hours.

Concerning the biochemical analysis methods it has to be mentioned that isolation and normalisation of lung samples for ROS measurement require considerate handling and very precise execution of the preparatory steps, since there usually is no option for automation. During the sample preparation steps, a human failure factor has to be considered, since not all steps could become time-coordinated precisely. Also, it has to be

considered that a relatively long time has passed between the harvesting of lung tissue and the actual measurement of free ROS production in tissue lysates. It included snap freezing, defrosting and a multi step preparation process and took approximately 1:30 to 2 hours at normoxic room air. There is a possibility that intracellular regulation of free ROS production happens within this time frame and therefore the immediate impact of hyperoxia can not be measured with the protocol applied in my experiments. With technical advances, maybe *in vivo* detection will become more widely available and can help to get clearer results on this matter. The assessed antioxidant defence enzymes are only an arbitrary selection representative for a whole complex enzymatic system, and therefore their singular expression's effect should not be generalized. For example, I did not consider analysing the EC-SOD which is preventing extracellular damage from ROS molecules, but primary damage was later seen in the extracellular matrix [65]. And finally, I measured the voluntary but not the maximal exercise capacity of mice in the running wheel assessment, thereby they did not reach the full performance capacity. Nevertheless, sportive activity did not undergo a specific training effect and was lacking external stimuli as occur in voluntary sportive exercise in humans.

5.4 Conclusion and outlook

In the presented mouse model, the sole postnatal administration of elevated FiO_2 -levels did neither cause the expected down-regulation of intrinsic free ROS production nor the up-regulation of antioxidant enzyme expression. But it seemed to induce more complex mechanisms. Voluntary physical activity later in life was not affected by postnatal oxygen treatment in mice, who show a high activity level in general. This could partly be due to a higher pulmonary regeneration capacity of mice. In this case, it would be important to understand why it is different to humans and how this difference can be transferred to the human situation in future investigations. These findings again underline the assumption that post-ventilation injury has multifactorial causes and only addressing them all can promise successful treatment and prevention of long-term damage. My findings give an idea and definitely motivate for further investigations using higher numbers of individuals and prospectively could even encourage human studies into this topic. Especially the results concerning intracellular antioxidant enzymes promise a relevant lead to eventual understanding of complex antioxidant defence mechanisms. A broader variety of intracellular as well as extracellular enzymes should be analysed to help explain the tendency of changes to free ROS formation following hyperoxia. Also, further investigations should aim at looking into more immediate assessment of cellular processes after hyperoxia.

6. Summary

With advanced medical treatment options, extremely preterm birth and associated complications become more and more relevant. Oxygen administration is frequently used to support the most vulnerable organ system of preterm neonates, the lung. But hyperbaric oxygen treatment carries manifold risks, including tissue damage due to increased levels of intracellular ROS. It is unknown to what extent postnatal hyperoxia changes intracellular mechanisms regarding free ROS formation and expression of antioxidant defence enzymes, as well as voluntary physical activity in adulthood. The analysis of these possible changes was the aim of this thesis.

A mouse model was used, in which newborns were postnatally exposed to moderate or severe hyperoxia for short or long durations and compared to untreated peers. Assessments were done either directly after hyperoxia in newborn or infant mice, or at the time the mice reached adulthood. The analysis of free ROS production in lung tissue was performed via EPR technology, the expression of a selection of antioxidant enzymes was analysed via immunoblot technique. Additionally, physical development and voluntary activity was recorded over the time of assessment.

It has been found that base free ROS formation in lung tissue is dependent on age and cellular compartment. A possible negative effect of external hyperoxia on intrinsic free ROS formation took a minimum of 120 min of oxygen treatment to be significant. Only moderate long-term postnatal hyperoxia showed an initial reduction of intracellular free ROS production, followed by an increase in adulthood. Adversely, severe postnatal hyperoxia did not show a comparable effect. The cellular expression rate of specific antioxidant defence enzymes in lung tissue changed with ageing and slightly with long-term oxygen treatment. Only MnSOD and catalase showed a relevant up-regulation due to hyperoxia during infancy, which returned to normal by reaching adulthood. The assessment of oxygen treatment-related impact on antioxidant enzymes did not sufficiently explain that on free ROS formation. Physical development and voluntary physical activity were not relevantly affected by perinatal hyperoxia.

In this murine study the expected negative effects of postnatal hyperoxia on intracellular mechanisms as well as voluntary physical activity were not reproducible. This can be due to differences between mice and humans and demonstrates the complexity of antioxidant mechanisms. Further investigation into the harm of hyperbaric oxygen treatment are needed.

7. Literature

1. Smith LJ, McKay KO, van Asperen PP, Selvadurai H, Fitzgerald DA (2010) Normal development of the lung and premature birth. *Paediatr Respir Rev* 11(3):135–142.
2. Narayanan M, Owers-Bradley J, Beardsmore CS, Mada M, Ball I, Garipov R, Panesar KS, Kuehni CE, Spycher BD, Williams SE, Silverman M (2012) Alveolarization continues during childhood and adolescence. New evidence from helium-3 magnetic resonance. *Am J Respir Crit Care Med* 185(2):186–191.
3. Chao C-M, El Agha E, Tiozzo C, Minoo P, Bellusci S (2015) A breath of fresh air on the mesenchyme. Impact of impaired mesenchymal development on the pathogenesis of bronchopulmonary dysplasia. *Front Med (Lausanne)* 2:27.
4. Speer CP (2011) Neonatal respiratory distress syndrome. An inflammatory disease? *Neonatology* 99(4):316–319.
5. Blencowe H, Cousens S, Oestergaard MZ, Chou D, Moller A-B, Narwal R, Adler A, Vera Garcia C, Rohde S, Say L, Lawn JE (2012) National, regional, and worldwide estimates of preterm birth rates in the year 2010 with time trends since 1990 for selected countries. A systematic analysis and implications. *The Lancet* 379(9832):2162–2172.
6. Hasselager AB, Børch K, Pryds OA (2016) Improvement in perinatal care for extremely premature infants in Denmark from 1994 to 2011. *Dan Med J* 63(1):A5182
7. Cherian S, Morris I, Evans J, Kotecha S (2014) Oxygen therapy in preterm infants. *Paediatr Respir Rev* 15(2):135–141.
8. Torres-Cuevas I, Cernada M, Nuñez A, Escobar J, Kuligowski J, Chafer-Pericas C, Vento M (2016) Oxygen Supplementation to Stabilize Preterm Infants in the Fetal to Neonatal Transition. No Satisfactory Answer. *Front Pediatr* 4:29.
9. Zeitlin J, Mohangoo A, Delnord M (May 2013a) European Perinatal Health Report 2010 - Euro-Peristat
10. Zeitlin J, Mohangoo AD, Delnord M, Cuttini M (2013b) The second European Perinatal Health Report. Documenting changes over 6 years in the health of mothers and babies in Europe. *J Epidemiol Community Health* 67(12):983–985.
11. Eber E, Zach MS (2001) Long term sequelae of bronchopulmonary dysplasia (chronic lung disease of infancy). *Thorax* 56(4):317–323
12. Bouch S, O'Reilly M, Harding R, Sozo F (2015) Neonatal exposure to mild hyperoxia causes persistent increases in oxidative stress and immune cells in the lungs

- of mice without altering lung structure. *Am J Physiol Lung Cell Mol Physiol* 309(5):L488-96.
13. Sena LA, Chandel NS (2012) Physiological roles of mitochondrial reactive oxygen species. *Mol Cell* 48(2):158–167.
 14. Cotton RB, Sundell HW, Zeldin DC, Morrow JD, Roberts LJ, Hazinski TA, Law AB, Steele S (2006) Inhaled nitric oxide attenuates hyperoxic lung injury in lambs. *Pediatr Res* 59(1):142–146.
 15. Das KC, Wasnick JD (2014) Biphasic response of checkpoint control proteins in hyperoxia. Exposure to lower levels of oxygen induces genome maintenance genes in experimental baboon BPD. *Mol Cell Biochem* 395(1-2):187–198.
 16. Solberg R, Andresen JH, Escrig R, Vento M, Saugstad OD (2007) Resuscitation of hypoxic newborn piglets with oxygen induces a dose-dependent increase in markers of oxidation. *Pediatr Res* 62(5):559–563. doi:10.1203/PDR.0b013e318156e8aa
 17. Frank L, Groseclose EE (1984) Preparation for birth into an O₂-rich environment. The antioxidant enzymes in the developing rabbit lung. *Pediatr Res* 18(3):240–244.
 18. Hilgendorff A, Reiss I, Ehrhardt H, Eickelberg O, Alvira CM (2014) Chronic lung disease in the preterm infant. Lessons learned from animal models. *Am J Respir Cell Mol Biol* 50(2):233–245.
 19. Amy RW, Bowes D, Burri PH, Haines J, Thurlbeck WM (1977) Postnatal growth of the mouse lung. *J Anat* 124(Pt 1):131–151
 20. Schneider H (2011) Oxygenation of the placental-fetal unit in humans. *Respir Physiol Neurobiol* 178(1):51–58.
 21. Lim K, Wheeler KI, Gale TJ, Jackson HD, Kihlstrand JF, Sand C, Dawson JA, Dargaville PA (2014) Oxygen saturation targeting in preterm infants receiving continuous positive airway pressure. *J Pediatr* 164(4):730-736.e1.
 22. Bhandari V (2010) Hyperoxia-derived lung damage in preterm infants. *Semin Fetal Neonatal Med* 15(4):223–229.
 23. Kallet RH, Matthay MA (2013) Hyperoxic acute lung injury. *Respir Care* 58(1):123–141.
 24. Tataranno ML, Oei JL, Perrone S, Wright IM, Smyth JP, Lui K, Tarnow-Mordi WO, Longini M, Proietti F, Negro S, Saugstad OD, Buonocore G (2015) Resuscitating preterm infants with 100% oxygen is associated with higher oxidative stress than room air. *Acta Paediatr* 104(8):759–765.

25. Sies H (1985) *Oxidative Stress*. Elsevier Science, Burlington
26. Frank L, Bucher JR, Roberts RJ (1978) Oxygen toxicity in neonatal and adult animals of various species. *J Appl Physiol Respir Environ Exerc Physiol* 45(5):699–704.
27. Frank L (1991) Developmental aspects of experimental pulmonary oxygen toxicity. *Free Radical Biology and Medicine* 11(5):463–494.
28. Berkelhamer SK, Kim GA, Radder JE, Wedgwood S, Czech L, Steinhorn RH, Schumacker PT (2013) Developmental differences in hyperoxia-induced oxidative stress and cellular responses in the murine lung. *Free Radic Biol Med* 61:51–60.
29. Datta A, Kim GA, Taylor JM, Gugino SF, Farrow KN, Schumacker PT, Berkelhamer SK (2015) Mouse lung development and NOX1 induction during hyperoxia are developmentally regulated and mitochondrial ROS dependent. *Am J Physiol Lung Cell Mol Physiol* 309(4):L369-77.
30. O'Reilly M, Hansbro PM, Horvat JC, Beckett EL, Harding R, Sozo F (2014) Bronchiolar remodeling in adult mice following neonatal exposure to hyperoxia. Relation to growth. *Anat Rec (Hoboken)* 297(4):758–769.
31. Heldt GP, McIlroy MB, Hansen TN, Tooley WH (1980) Exercise performance of the survivors of hyaline membrane disease. *J Pediatr* 96(6):995–999
32. Mitchell SH, Teague WG (1998) Reduced gas transfer at rest and during exercise in school-age survivors of bronchopulmonary dysplasia. *Am J Respir Crit Care Med* 157(5 Pt 1):1406–1412.
33. Smith LJ, van Asperen PP, McKay KO, Selvadurai H, Fitzgerald DA (2008) Reduced exercise capacity in children born very preterm. *Pediatrics* 122(2):e287-93.
34. Winck AD, Heinzmann-Filho JP, Schumann D, Zatti H, Mattiello R, Jones MH, Stein RT (2016) Growth, lung function, and physical activity in schoolchildren who were very-low-birth-weight preterm infants. *J Bras Pneumol* 42(4):254–260.
35. van Haaften T, Byrne R, Bonnet S, Rochefort GY, Akabutu J, Bouchentouf M, Rey-Parra GJ, Galipeau J, Haromy A, Eaton F, Chen M, Hashimoto K, Abley D, Korbitt G, Archer SL, Thébaud B (2009) Airway delivery of mesenchymal stem cells prevents arrested alveolar growth in neonatal lung injury in rats. *Am J Respir Crit Care Med* 180(11):1131–1142.
36. da Cunha MJ, da Cunha AA, Ferreira GK, Baladão ME, Savio LEB, Reichel CL, Kessler A, Netto CA, Wyse ATS (2013) The effect of exercise on the oxidative stress induced by experimental lung injury. *Life Sci* 92(3):218–227.

37. Venditti P, Di Meo S (1997) Effect of training on antioxidant capacity, tissue damage, and endurance of adult male rats. *Int J Sports Med* 18(7):497–502.
38. Wang X, Fang H, Huang Z, Shang W, Hou T, Cheng A, Cheng H (2013) Imaging ROS signaling in cells and animals. *J Mol Med* 91(8):917–927.
39. Halliwell B (1978) Superoxide-dependent formation of hydroxyl radicals in the presence of iron chelates. Is it a mechanism for hydroxyl radical production in biochemical systems? *FEBS Lett* 92(2):321–326
40. Halliwell B, Gutteridge JM (1990) Role of free radicals and catalytic metal ions in human disease. An overview. *Meth Enzymol* 186:1–85
41. Brand MD (2016) Mitochondrial generation of superoxide and hydrogen peroxide as the source of mitochondrial redox signaling. *Free Radic Biol Med* 100:14–31.
42. Al-Gubory KH, Fowler PA, Garrel C (2010) The roles of cellular reactive oxygen species, oxidative stress and antioxidants in pregnancy outcomes. *Int J Biochem Cell Biol* 42(10):1634–1650.
43. Cai H, Dikalov S, Griendling KK, Harrison DG (2007) Detection of reactive oxygen species and nitric oxide in vascular cells and tissues. Comparison of sensitivity and specificity. *Methods Mol Med* 139:293–311
44. Finkel T (1998) Oxygen radicals and signaling. *Current Opinion in Cell Biology* 10(2):248–253.
45. Sies H, Berndt C, Jones DP (2017) Oxidative Stress. *Annu Rev Biochem* 86:715–748.
46. Mittal M, Siddiqui MR, Tran K, Reddy SP, Malik AB (2014) Reactive oxygen species in inflammation and tissue injury. *Antioxid Redox Signal* 20(7):1126–1167.
47. Pérez-Torres I, Guarner-Lans V, Rubio-Ruiz ME (2017) Reductive Stress in Inflammation-Associated Diseases and the Pro-Oxidant Effect of Antioxidant Agents. *Int J Mol Sci* 18(10).
48. McCord JM, Fridovich I (1969) Superoxide dismutase. An enzymic function for erythrocyte hemocuprein (hemocuprein). *J Biol Chem* 244(22):6049–6055
49. Nozik-Grayck E, Dieterle CS, Piantadosi CA, Enghild JJ, Oury TD (2000) Secretion of extracellular superoxide dismutase in neonatal lungs. *Am J Physiol Lung Cell Mol Physiol* 279(5):L977-84.
50. Nicco C, Batteux F (2017) ROS Modulator Molecules with Therapeutic Potential in Cancers Treatments. *Molecules* 23(1).

51. Valencia AM, Abrantes MA, Hasan J, Aranda JV, Beharry KD (2018) Reactive Oxygen Species, Biomarkers of Microvascular Maturation and Alveolarization, and Antioxidants in Oxidative Lung Injury. *React Oxyg Species (Apex)* 6(18):373–388.
52. Davis JM, Auten RL (2010) Maturation of the antioxidant system and the effects on preterm birth. *Semin Fetal Neonatal Med* 15(4):191–195.
53. Georgeson GD, Szőny BJ, Streitman K, Varga IS, Kovács A, Kovács L, László A (2002) Antioxidant enzyme activities are decreased in preterm infants and in neonates born via caesarean section. *European Journal of Obstetrics & Gynecology and Reproductive Biology* 103(2):136–139.
54. Qanungo S, Mukherjea M (2000) Ontogenic profile of some antioxidants and lipid peroxidation in human placental and fetal tissues. *Mol Cell Biochem* 215(1-2):11–19
55. Halliwell B, Gutteridge JMC, Aruoma OI (1987) The deoxyribose method. A simple “test-tube” assay for determination of rate constants for reactions of hydroxyl radicals. *Analytical Biochemistry* 165(1):215–219.
56. Zhao H, Kalivendi S, Zhang H, Joseph J, Nithipatikom K, Vásquez-Vivar J, Kalyanaraman B (2003) Superoxide reacts with hydroethidine but forms a fluorescent product that is distinctly different from ethidium. Potential implications in intracellular fluorescence detection of superoxide. *Free Radic Biol Med* 34(11):1359–1368
57. Aguilera-Venegas B, Speisky H (2014) Identification of the transition state for fast reactions. The trapping of hydroxyl and methyl radicals by DMPO-A DFT approach. *J Mol Graph Model* 52:57–70.
58. Shvedova AA, Kisin ER, Murray AR, Mouithys-Mickalad A, Stadler K, Mason RP, Kadiiska M (2014) ESR evidence for in vivo formation of free radicals in tissue of mice exposed to single-walled carbon nanotubes. *Free Radic Biol Med* 73:154–165.
59. Dikalov S, Skatchkov M, Bassenge E (1997) Spin trapping of superoxide radicals and peroxynitrite by 1-hydroxy-3-carboxy-pyrrolidine and 1-hydroxy-2,2,6, 6-tetramethyl-4-oxo-piperidine and the stability of corresponding nitroxyl radicals towards biological reductants. *Biochem Biophys Res Commun* 231(3):701–704.
60. Adam S, Loertzer H, Fornara P, Brömme HJ (2010) The carboxyproxyl-derived spin trap (CP-H) is an appropriate detector-compound for oxidative stress. *Urol Res* 38(3):179–186.

61. Meijer JH, Robbers Y (2014) Wheel running in the wild. *Proc Biol Sci* 281(1786).
62. Bartling B, Al-Robaiy S, Lehnich H, Binder L, Hiebl B, Simm A (2017) Sex-related differences in the wheel-running activity of mice decline with increasing age. *Exp Gerontol* 87(Pt B):139–147.
63. Frezza C, Cipolat S, Scorrano L (2007) Organelle isolation. Functional mitochondria from mouse liver, muscle and cultured fibroblasts. *Nat Protoc* 2(2):287–295.
64. Kuchnicka K, Maciejewski D (2013) Ventilator-associated lung injury. *Anaesthesiol Intensive Ther* 45(3):164–170.
65. Kindermann A, Binder L, Baier J, Gündel B, Simm A, Haase R, Bartling B (2019) Severe but not moderate hyperoxia of newborn mice causes an emphysematous lung phenotype in adulthood without persisting oxidative stress and inflammation. *BMC Pulm Med* 19(1):245.
66. Kneyber MCJ, Luca D de, Calderini E, Jarreau P-H, Javouhey E, Lopez-Herce J, Hammer J, Macrae D, Markhorst DG, Medina A, Pons-Odena M, Racca F, Wolf G, Biban P, Brierley J, Rimensberger PC (2017) Recommendations for mechanical ventilation of critically ill children from the Paediatric Mechanical Ventilation Consensus Conference (PEMVECC). *Intensive Care Med* 43(12):1764–1780.

8. Theses

1. Intracellular free ROS production is mainly performed within the mitochondria-reduced cytoplasm and dependent on the age of individuals.
2. Short-term moderate or severe hyperoxia causes a down-regulation of intracellular free ROS formation only after 120 min of oxygen treatment.
3. Only moderate long-term postnatal hyperoxia has an effect on intracellular free ROS formation, showing an initial postinterventional decrease followed by an increase of ROS production later in adulthood compared to untreated peers.
4. Cellular expression levels of antioxidant enzymes in lung tissue depend on the specific enzyme, the age of individuals and are only influenced by postnatal hyperoxia during infancy.
5. Postnatal moderate or severe hyperoxia has no relevant effect on murine physical development and voluntary physical exercise capacity later in adulthood.

Erklärungen

(1) Erklärung zum Wahrheitsgehalt der Angaben und frühere Promotionsversuche

Ich erkläre, die Angaben wahrheitsgemäß gemacht und bisher keinen Promotionsversuch unternommen zu haben, sowie dass kein Promotionsverfahren an einer anderen wissenschaftlichen Einrichtung läuft.

(2) Eidesstattliche Erklärung

Ich erkläre an Eides statt, dass ich die Arbeit selbstständig und ohne fremde Hilfe verfasst habe. Alle Regeln der guten wissenschaftlichen Praxis wurden eingehalten; es wurden keine anderen als die von mir angegebenen Quellen und Hilfsmittel benutzt und die den benutzten Werken wörtlich oder inhaltlich entnommenen Stellen als solche kenntlich gemacht. Die vorliegende wissenschaftliche Arbeit wurde an keiner anderen wissenschaftlichen Einrichtung im In- und Ausland in gleicher oder ähnlicher Form einer Prüfungsbehörde vorgelegt.

Bremen, den 07.05.2021



Leonore Binder

Danksagung

Ich danke der Klinik für Herzchirurgie für die Annahme als Doktorandin und Bereitstellung der Forschungsräumlichkeiten, insbesondere Herrn Prof. Dr. Simm als Leiter der Forschungsabteilung. Herrn Dr. HJ Brömme danke ich für die Einführung in das EPR System auch über den Ruhestand hinaus - sein besonderer Einsatz machte die Nutzung dieser selten genutzten Messmethode erst möglich. Ich danke Herrn PD Dr. Hiebl als Tierschutzbeauftragtem für die Vermittlung einer Sondergenehmigung für meine experimentelle Tätigkeit, sowie Herrn Dr. Lehnich für die Erarbeitung, Ausführung und technische Betreuung des Laufradsystems.

Während der laborexperimentellen Phase wurde ich vom gesamten Team des HTC-Forschungslabors und des Zentrums für medizinische Grundlagenforschung (ZMG) großartig betreut und in die Laborarbeit eingewiesen, vielen Dank dafür. Insbesondere an die MTA Frau Glaubitz, Frau Dr. Al-Robaiy, Herrn Dr. Navarrete-Santos, sowie allen zu diesem Zeitpunkt anwesenden Doktorandinnen und Doktoranden, die mir stets mit Rat und Tat zur Seite standen. Ich danke außerdem Frau Beate Gründel, die im Rahmen ihrer Bachelorarbeit das verwendete EPR-Protokoll für unsere Arbeitsgruppe ausgearbeitet und angepasst hat. Frau Anke Kindermann danke ich herzlich für die intensive Betreuung, geduldige Anleitung und bereitwillige Beratung, sowie klaglose Wiederholung alles Gesagten auch über die gemeinsame experimentelle Phase hinaus.

Mein besonderer Dank gilt meiner Betreuerin, Frau PD Dr. Babett Bartling, für die Überlassung des Themas, sowie ihre kompetente Unterstützung bei der Planung und Erarbeitung der Experimente und der Strukturierung der Dissertation. Ich habe in ihr allzeit eine zugewandte und bereitwillige Ansprechpartnerin gefunden, die über das von ihr erwartete Soll hinaus ohne Zeitverzug sowohl inhaltlich als auch formell großartige Anregungen brachte.

Nicht zuletzt gilt mein Dank meiner Familie und meinem Freundeskreis, welche mich jederzeit unterstützten und geduldig waren, durch gezieltes Nachfragen aber auch die Motivation aufrecht erhielten und mich dabei weit über die Approbation hinaus begleiteten.